TNO Built Environment and Geosciences

TNO report

TNO-034-UT-2009-02065

Terschelling Basin and southern Dutch Central Graben
Burial history, temperature, source rock maturity and hydrocarbon generation - Area 2A

Date	1 October 2009
Author(s)	J.M. Verweij
	M. Souto Carneiro Echternach
	N. Witmans
Assignor	
Project number	034.20779 THEMAKAR
Number of pages	46 (excl. appendices)
Number of appendices	6

Contents

1 Introduction

1.1 Mapping of the deep subsurface of the Netherlands offshore (NCP-2 project)

The detailed mapping of seven offshore areas on the Netherlands Continental Shelf was initiated in late 2005 and will be finalised in 2010. It builds on and goes one step beyond the previous regional mapping of the Netherlands onshore and offshore. In 2004 the publication of the Geological Atlas of the Subsurface of the Netherlands – *onshore* rounded off the onshore regional mapping project and a 'quick and dirty' offshore mapping (NCP-1 project) was completed in 2006 (viz. on the http://www.nlog.nl; Duin et al., 2006).

The main aim of the detailed mapping of seven sub-areas is to present a more comprehensive model of the subsurface to future and current operators in the oil industry and to governmental and non-governmental organisations for, amongst other things, the spatial planning of the Dutch subsurface. The deliverables include:
3D geological framework (depth and thickness grids)
Rock and fluid parameters (petro physical parameters, P, T, Vr)
3D burial histories
Petroleum system analysis
All deliverables, such as maps, grids and graphs, can be downloaded at the http://www.nlog.nl site. When applicable, regular updates will be made available on the site.

1.2 Definition of mapping areas in the Netherlands offshore

Based on consultation with the exploration departments of the oil companies operating in the Netherlands it was decided to divide the offshore area into seven sub-areas (Figure 1). These areas represent more or less structural entities at the Late Jurassic to Early Cretaceous times (Figure 2). The detailed mapping project started with sub-area NCP-2A: Terschelling Basin and the southern part of the Dutch Central Graben (Figure 2).

1.3 Detailed mapping of the Terschelling Basin and southern part of the Dutch Central Graben

The detailed mapping was focussed on the assessment of the present-day stratigraphic and structural framework of the sedimentary fill of the area as well as on the properties of rocks and fluids it contains, such as reservoir porosity, pore fluid pressure, formation water salinity, source rock maturity, characteristics of oil and gas. Special attention was paid to improve the lithostratigraphic sub-division of the complex Upper Jurassic sequence, and to provide new porosity data for the main reservoir units in the Upper Rotliegend Group, Germanic Trias groups and the Schieland Group. 3D basin modelling was used to integrate the data, visualise the geodynamic, geothermal and geofluid history the area, and herewith to provide additional information of importance for evaluating the petroleum systems.
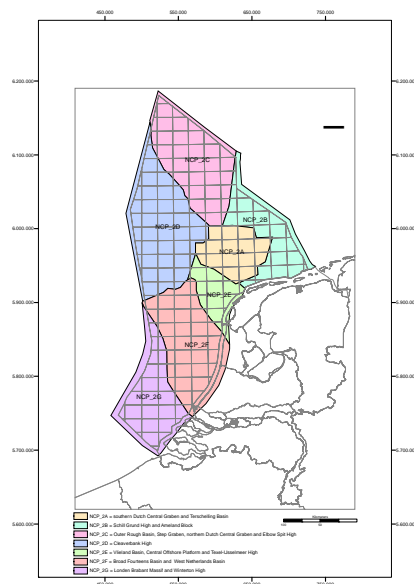
Figure 1. NCP-2 areas, including the location of the project area NCP-2A.
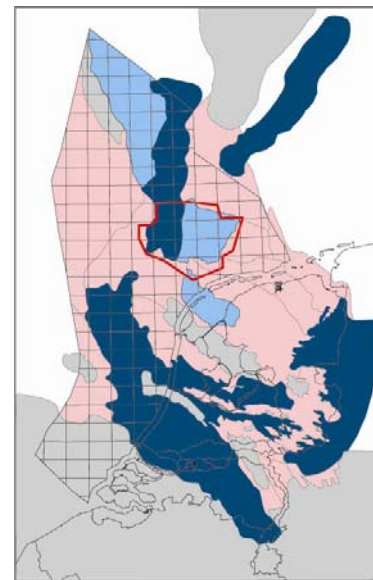
Figure 2. Structural setting at Late Jurassic-Early Cretaceous. Location of the project area NCP-2A (in red): Terschelling Basin and southern part of the Dutch Central Graben.

1.4 Geological setting Terschelling Basin and southern part of the Dutch Central Graben

The dominant features of the present-day structural framework and lithostratigraphic build-up of the area (Figure 3) reflect its complex geodynamic history. Important phases of this geodynamic history include the Saalian phase of uplift and erosion, Mid-Kimmerian phase of erosion, Late Jurassic-Early Cretaceous rifting and Sub-Hercynian inversion phase. The main structural elements in the area are: the Dutch Central Graben and Terschelling Basin, as well as the adjacent Central Offshore Platform, Vlieland
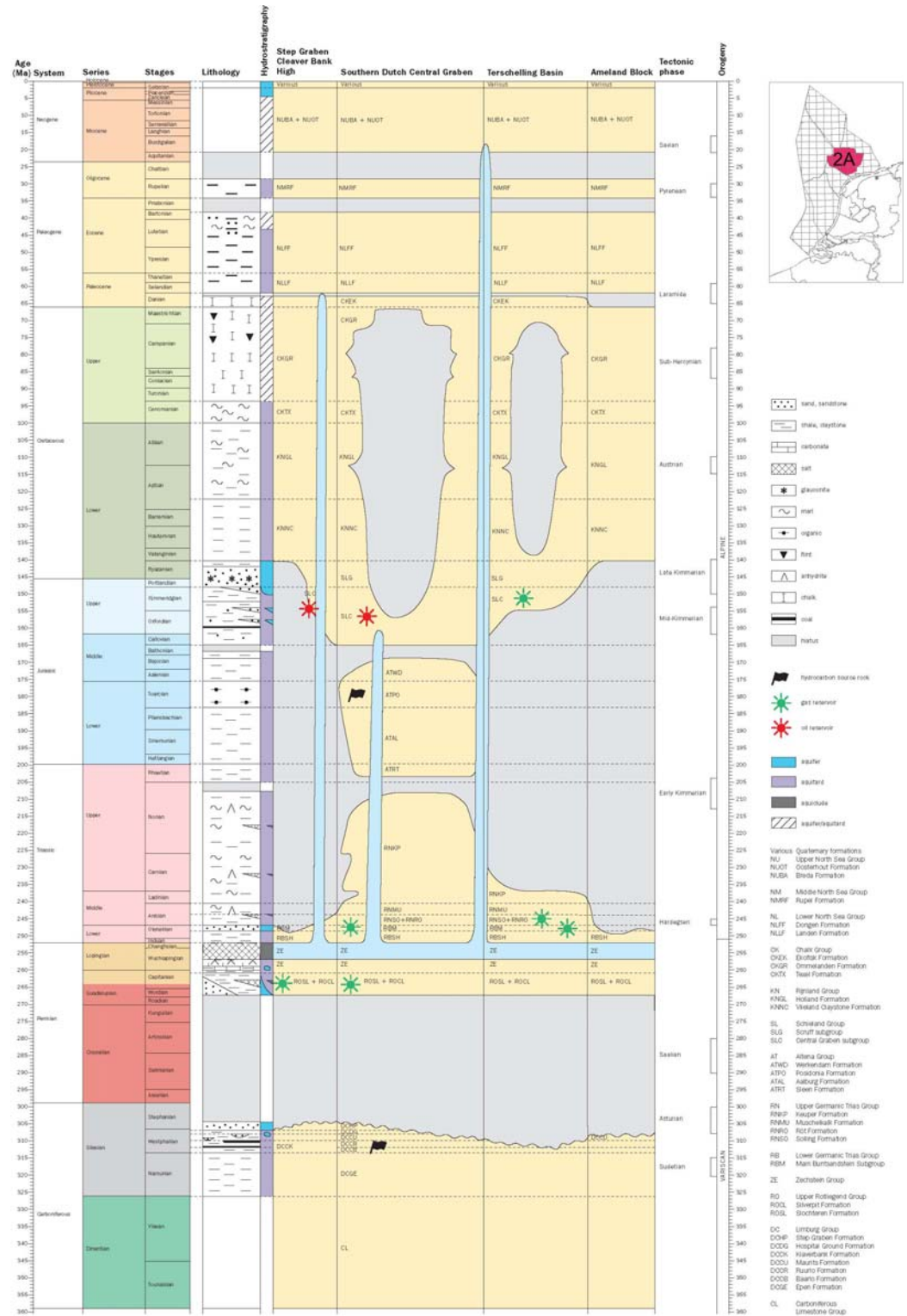
Tectono-stratigraphic chart of the Dutch Central Graben and Terschelling Basin. Time scale according to Gradstein et al. (2004).
The subdivision of the Upper Jurassic presented here does not follow the official stratigraphic nomenclature of the Netherlands (Adrichem Boogaert
& Kouwe, 1997). In this study the Schieland Group (SL) is subdivided into the Scruff subgroup (SLG) and the Central Graben subgroup (SLC).
The Scruff subgroup relates to the former Scruff Group while the Central Graben subgroup relates to the former Schieland Group.

Figure 3.   Tectonostratigraphic chart of the southern part of the Dutch Central Graben and the Terschelling Basin.

High and Ameland Block, and the northwestern extension of the Lauwerszee Trough
that reaches the southern border of the area (Figure 4). Some of these structures are of
Carboniferous origin and regained importance in Mesozoic times.

The presence of Zechstein evaporites greatly influenced the post-Permian structural and
sedimentary development of the area. The original estimated thickness depositional
thickness of the Zechstein Group was c. 650 m, while its present-day thickness varies
from approximately 5000 m to only a few metres in withdrawal areas. The circa 30
identified salt structures follow the structural grain of the area. Timing of salt
movement is related to phases of active fault movement. Halokinesis occurred during
different phases of geological history and started already in the Early and Middle
Triassic.
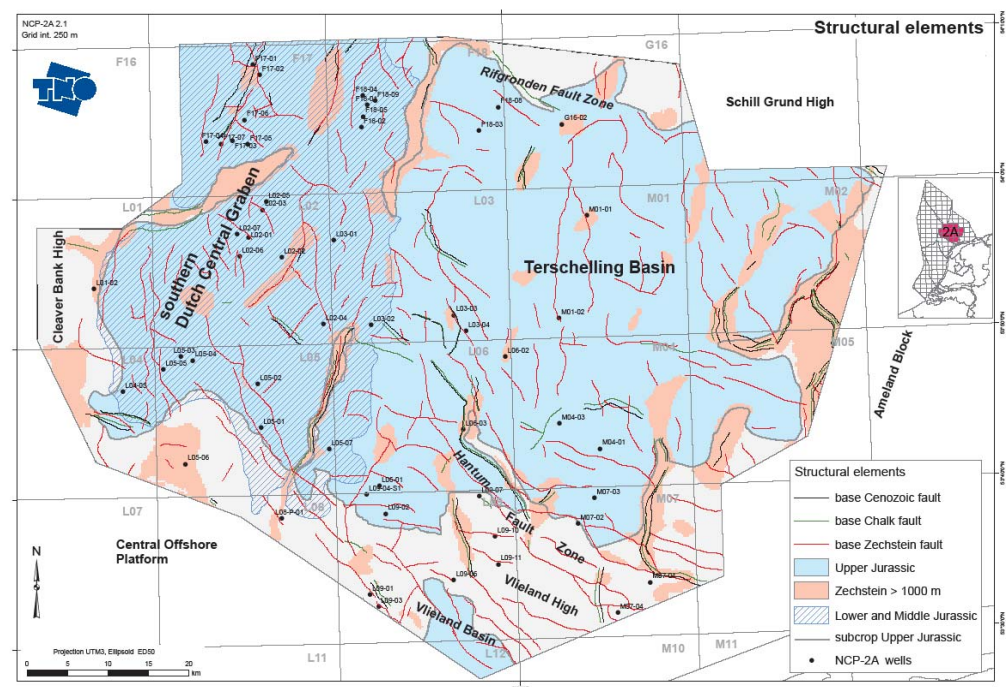
Figure 4. Structural elements and salt structures.

Figure 5 shows the distribution of the oil and gas fields in the area. The main source
rocks for gas are the coal measures of the Limburg Group. These source rocks of
kerogen type III include the Baarlo Formation, Ruurlo and the Maurits Formation. The
occurrence of the Maurits Formation is probably restricted to the southwestern part of
the area. Coal layers in the Central Graben Subgroup (Schieland Group) are considered
to be secondary source rocks for gas. The Posidonia Shale Formation is the main source
rock for oil. The present-day distribution of this source rock of kerogen type II is
restricted to the southern part of the Dutch Central Graben. Possible additional source
horizons occur in the Aalburg and Sleen Formations of the Altena Group (De Jager and
Geluk, 2007).

Detailed information on the present-day stratigraphic and structural framework of the
sedimentary fill of the area and the properties of the rocks and fluids it contains, such as
porosities, pressures, salinities, characteristics of oil and gas, are presented in Verweij
and Witmans (2009).
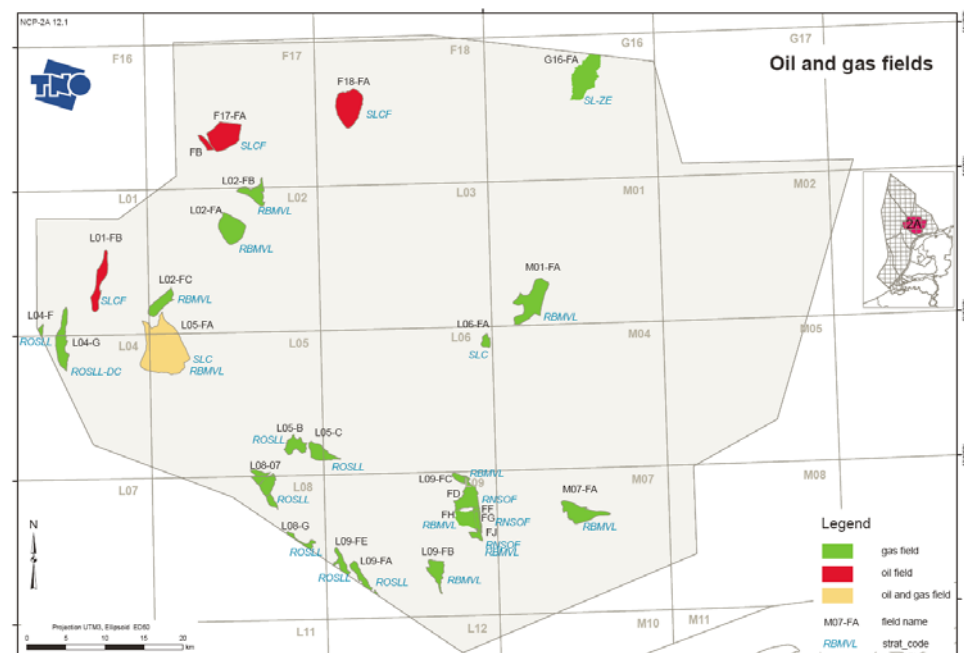
Figure 5. Oil and gas fields in the Terschelling Basin and Dutch Central Graben.

1.5 Basin modelling Terschelling Basin and southern part of the Dutch Central Graben

TNO uses 1D, 2D and 3D basin modelling (Petromod, version 10, of IES/Schlumberger) to integrate the wealth of data and information gathered and mapped in its detailed mapping programme of subareas of offshore Netherlands and to evaluate the interdependencies of the different processes that affect rocks and fluids during its geological history. Special attention is paid to processes and conditions affecting hydrocarbon potential. Here we present selected results from a full 3D reconstruction of the burial history, and the history of temperature, source rock maturity and timing of hydrocarbon generation in the Terschelling Basin and southern part of the Dutch Central Graben from 320 Ma to present-day.

2 Basin modelling: Workflow, input data and boundary conditions

2.1 Assumptions and conditions underlying the basin modelling approach

General assumptions and conditions inherent in basin modelling:

- Geological history:
  - o the model is laterally constrained: no horizontal compression or extension of the basin fill is taken into account
  - o vertical movement only (no lateral deformation of the sediments in the model, except for salt movement)
  - o salt movement has no direct relation to changes in stress
  - o compaction of the basin fill is vertical
  - o compaction is mechanical according to vertical effective stress-based rock property model
- History pore water fluids
  - o density of pore water is constant
- Thermal history
  - o conductive heat flow

The basin modelling scenarios presented here are based on a geological model without faults and hydrostatic conditions are assumed in all scenarios.
In addition to the above listed general limiting assumptions and conditions, default set-ups of the modelling package influence simulation results. Such default set-ups include default relations between standard lithologies and properties through compaction approaches, porosity-permeability relations, thermal models, kinetic models ; mixing rules lithology. The selection of the proper set-up is an important part of the basin modelling workflow.

2.2 Data base

The basic data requirements for the 3D modelling involve: present-day geometry (stratigraphy; property/facies boundaries within stratigraphic units, water depth); lithological properties (lithological composition of each stratigraphic unit and eroded – part of – unit and of each facies); quantified uninterrupted time-sequence of events during geological history (3D history of sedimentation, uplift and erosion; estimated thickness of erosion; 3D history of water depth, basal heat flow, surface temperature; timing of salt movement); calibration data (such as present-day temperatures, porosities, permeabilities, pressures, vitrinite reflectance measurements).
The results of the detailed mapping of the Terschelling Basin and the southern part of the Dutch Central Graben (Verweij and Witmans, 2009) provided the basic conceptual model of the geological evolution and the input data and calibration data required for the numerical modelling.

2.3 Basin modelling workflow

Initially 1D simulations at about 30 well locations were carried out to verify the conceptual models of subsidence and erosion history.

The general workflow with respect to the full 3D basin modelling of the Terschelling Basin and Dutch part of the Central Graben, as decribed here, included the following steps:
Building 3D geological model;
Selection proper Petromod default porosity-depth and porosity-permeability relations;
Running 3D model for reconstructing burial history;
Selection proper thermal conductivity model (using measured temperature data and published information on thermal conductivities); the default Sekiguchi model of Petromod was selected;
Running 3D model for reconstructing history of temperature and source rock maturity (using kinetic model Sweeney and Burnham, 1990 and a constant basal heat flow boundary condition of 60 mW/m^2);
Running 3D model for reconstructing history of temperature and source rock maturity (using kinetic model Sweeney and Burnham, 1990 and tectonic heat flow boundary condition from Abdul Fattah et al., 2008);
Comparison of model runs 5 and 6 and selection basal heat flow boundary condition;

Running 3D model for reconstructing the history of temperature, source rock maturity and timing of hydrocarbon generation, using the Burnham (1989)_T2 kinetic model for the Posidonia Shale Formation and Burnham (1989)_T3 kinetic model for the Carboniferous source rocks and tectonic heat flow boundary condition, and a set of source rock parameters, see Table 3;
Evaluation simulation results.

2.4 Input: Present-day geometry

The present-day 3D stratigraphic model was the basic input for the 3D modelling. Depth and thickness maps of 11 stratigraphic groups (Upper North Sea, Lower & Middle North Sea, Chalk, Rijnland, Scruff, Schieland, Altena, Upper Germanic Trias, Lower Germanic Trias, Zechstein and Rotliegend groups) were loaded from Petrel into Petromod and horizons were adjusted. The present-day model was refined with additional maps of two reservoir units (Lower Detfurth Sandstone Member, Lower Volpriehausen Sandstone Member) and one source rock (Posidonia Shale Formation). Layers were split to include additional reservoir and sealing units (Solling Formation reservoir and the sealing evaporites of the Röt Formation in the Upper Germanic Trias Group; Terschelling Sandstone Formation reservoir in the Schieland Group), and to facilitate the inclusion of erosional phases (splitting of Chalk Group).

Facies maps were created to take lateral facies changes into account (Upper Rotliegend Group; Solling Formation). The stratigraphic model was extended until greater depth with the Step Graben & Hospital Ground, Maurits, Ruurlo and Baarlo formations of the Limburg Group. Maps with estimated present-day thicknesses were incorporated in the model: 0 – 250 m for the Step Graben & Hospital Ground, 0 – 200 m for the Maurits, 0 – 400 m for the Ruurlo and 100 – 200 m for the Baarlo formations. The 3D model includes 29 layers plus basement (Figure 6, Table 1) (the stratigraphic input model was used for simulation calculations; the output sampled grid contains 126 990 gridnodes).
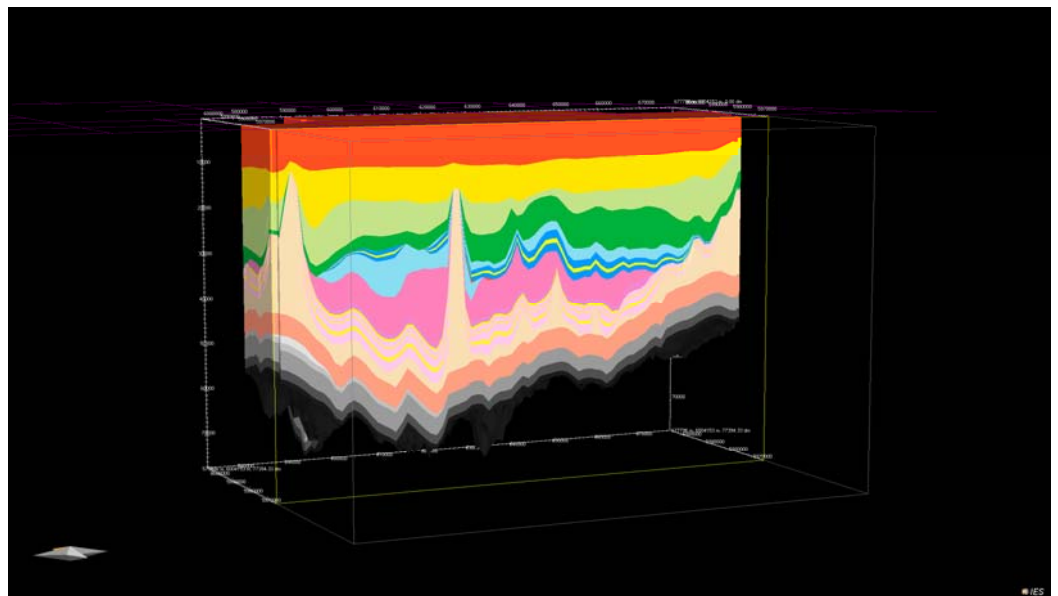

Figure 6. Present-day 3D geometrical model of the Dutch Central Graben and Terschelling Basin.

2.5 Input: Properties

Lithology: Lithological compositions were assigned to each layer. Facies changes were assigned to the bottom layer of the Upper Germanic Trias Group and to the Upper Rotliegend Group (Tables 1 and 2).

Table 1. Model stratigraphy: 30 layers and assigned lithological composition in Terschelling Basin and Dutch Central Graben. Note difference in facies in layers 16, 24 and 25.

Layer	Lithology
	Facies
1 Upper North Sea Group_top	75%Sand 25%Shale
2 Upper North Sea Group_ bottom	75%Sand 25%Shale
3 Middle North Sea Group	75%Sand 25%Shale
4 Lower North Sea Group	100% Shale
5 Chalk Group_ top	100% Chalk
6 Chalk Group_bottom	100% Chalk
7 Rijnland Group	60% Shale 20% Silt 20% Marl
8 Schieland Group_Scruff subgroup	75% Shale 25%Silt
9 Schieland Group_top	75% Shale 25%Silt
10 Terschelling Sandstone Formation	100% Sand
11 Schieland Group_bottom	75% Shale 25%Silt
12 Posidonia Shale Formation	100% Shale
13 Altena Group	75% Shale 25%Silt
14 Upper Germanic Trias Group_top	50%Shale 25%Silt 25%Limestone
15 Upper Germanic Trias Group_ salt	100% Salt
16 Upper Germanic Trias Group_ bottom	50%Shale 25%Silt 25%Limestone; 100%Sand
17 Lower Germanic Trias Group_top	75% Shale 25%Silt
18 Lower Detfurth Sandstone Mbr	100% Sand
19 Lower Germanic Trias Group-middle	75% Shale 25%Silt
20 Lower Volpriehausen Sandstone Mbr	100% Sand
21 Lower Germanic Trias Group_bottom	75% Shale 25%Silt
22 Zechstein Group	100% Salt
23 Upper Rotliegend Group_top	75% Shale 25%Silt
24 Upper Rotliegend Group_middle	75% Shale 25%Silt; 60%Shale20%Silt15%Salt5%Lime
25 Upper Rotliegend Group_bottom	75% Shale 25%Silt; 100% Sand
26 Step Graben/Hospital Ground Fms	60%Sand 20%Silt 18%Shale 2%Coal
27 Maurits Formation	80%Shale 15%Sand 5%Coal
28 Ruurlo Formation	78%Shale 20%Sand 2%Coal
29 Baarlo Formation	48%Shale 25%Silt 25%Sand 2%Coal
30 Basement	Basement

Table 2. Regional variation in facies of the Upper Rotliegend Group (layers 24 and 25).

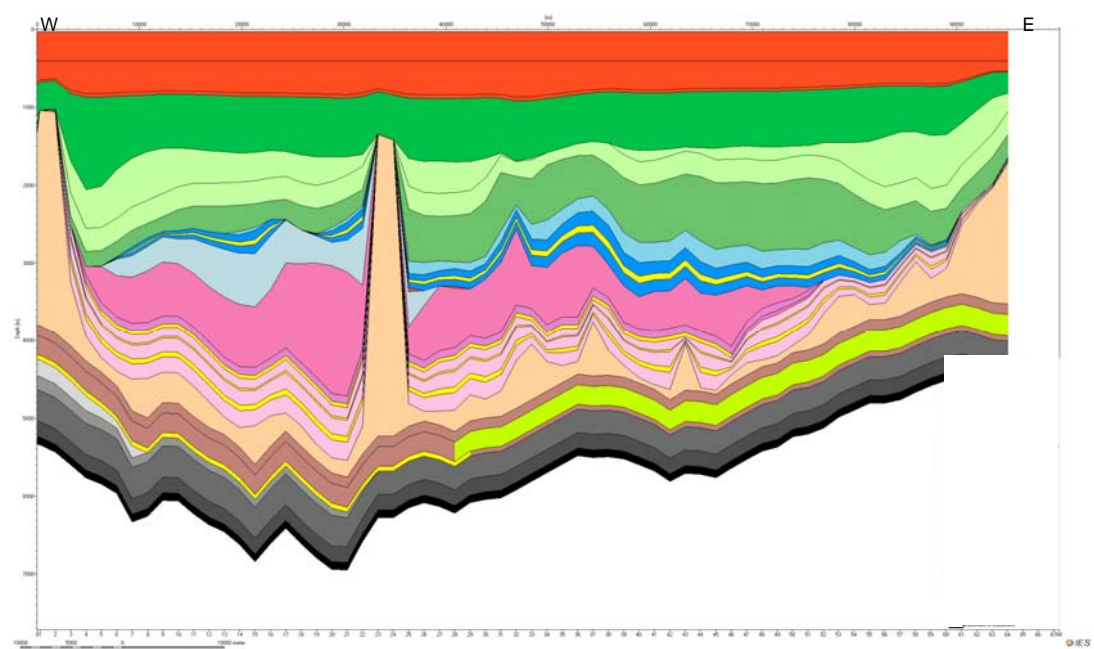| Layer	Lithology M04-03	Lithology L03-03	Lithology L05-03,L09-10
23 Upper Rotliegend Group_top	75% Shale 25%Silt	75% Shale 25%Silt	75% Shale 25%Silt
24 Upper Rotliegend Group_middle	75% Shale 25%Silt	60%Shale20%Silt15%Salt5%Lime	75% Shale 25%Silt
25 Upper Rotliegend Group_bottom	75% Shale 25%Silt	75% Shale 25%Silt	100% Sand

Figure 7. 2D extraction of the 3D facies model showing a W-E cross-section through the southern Dutch Central Graben and the Terschelling Basin (yellow: sandstone facies).

Source rock properties: The model includes two source rock intervals: the Carboniferous coal measures of the Limburg Group and the Posidonia Shale Formation. The gas prone coals of the Baarlo, Ruurlo and Maurits formations have been defined as source rocks of kerogen type III. The oil-prone Posidonia Shale Formation was assigned a source rock of kerogen type II. Table 3 shows measured characteristics of the source rocks and the source rock parameter values used for simulating the timing of hydrocarbon generation.

Table 3. Average source rock parameters measured at 22 wells and final set of source rock parameters used for simulating timing of hydrocarbon generation.

Source rock	Measured_TOC (wt%) average	TOC_input_PM (wt%)	Measured_HI (mgHC/gTOC)	HI_input_PM (mgHC/gTOC)
		final		*final*
Posidonia	9	9	579.22	600
Maurits	4.43	5	194.84	250
Ruurlo	10.75	2	64.33	250
Baarlo**	5.98	2	91.30	250

**TOC and HI values derived from wells in southern part Dutch North Sea

Pore water/formation water properties. In the model the pore water is of constant density, that is the density of the water is independent of changes in temperature and salinity. The water is incompressible.

Rock properties. The solid rock is incompressible. Salt is impermeable ($k = 10^{-16}$ mD).

2.6   Input: Quantified uninterrupted time-sequence of events

Table 4 shows the timing and duration of periods sedimentation, erosion and nondeposition from Late Carboniferous to present-day. The geological evolution includes the 3 main phases of erosion, namely the Saalian, Mid-Kimmerian and Sub-Hercynian phases, and additional periods of non-deposition, for example in the Tertiary (Figure 3).

Table 4. Timing and duration of periods of sedimentation, erosion and nondeposition.

Layer	Deposition age (Ma)		Erosion age (Ma)	
	From	To	From	To
1 Upper North Sea Group_top	1,81	0	0	0
2 Upper North Sea Group_ bottom	5,33	1,81	0	0
3 Middle North Sea Group	20,43	14,8	0	0
4 Lower North Sea Group	56,8	30,4	0	0
5 Chalk Group_ top	80	61,7	0	0
6 Chalk Group_bottom	99	83,5	83,5	80,5
7 Rijnland Group	140	99	80,5	80
8 Schieland Group_Scruff subgroup	145	140	0	0
9 Schieland Group_top	146,8	145	0	0
10 Terschelling Sandstone Formation	148	146,8	0	0
11 Schieland Group_bottom	154	148	0	0
12 Posidonia Shale Formation	183	176	173	172
13 Altena Group	203,6	183	172	162
14 Upper Germanic Trias Group_top	241	203,6	162	157
15 Upper Germanic Trias Group_ salt	243	241	157	156
16 Upper Germanic Trias Group_ bottom	245	243	156	154
17 Lower Germanic Trias Group_top	247,6	246,2	0	0
18 Lower Detfurth Sandstone Mbr	247,8	247,6	0	0
19 Lower Germanic Trias Group-middle	248,6	247,8	0	0
20 Lower Volpriehausen Sandstone Mbr	249	248,6	0	0
21 Lower Germanic Trias Group_bottom	254	249	0	0
22 Zechstein Group	258	254	0	0
23 Upper Rotliegend Group_top	260,85	258	0	0
24 Upper Rotliegend Group_middle	266,17	260,85	0	0
25 Upper Rotliegend Group_bottom	267,5	266,17	0	0
26 Step Graben/Hospital Ground Fms	308	300	300	292
27 Maurits Formation	310	308	292	288
28 Ruurlo Formation	312	310	288	280
29 Baarlo Formation	316,5	312	280	278
30 Basement	320	316,5	0	0

<u>Salt deformation</u>. Deformation of Zechstein salt is incorporated in the 3D simulations (not in the initial 1D simulations at well locations). The 'salt movement' tool of Petromod was used to simulate the movement of Zechstein salt, taking the calculated original thickness of the Zechstein Group as original depositional thickness. This original constant thickness of the Zechstein Group over the whole area was derived from the present-day volume of the Zechstein Group. The calculated original thickness of the Zechtein Group is 540 m. Salt movement was set to start in the Triassic. The 3D simulations did not take salt deformation of Upper Rotliegend and Upper Triassic evaporites into account.

Erosion. The 3D thickness of the eroded sediments was reconstructed for each main period of erosion. For that purpose, we first estimated the original thicknesses of missing stratigraphic units using the top Carboniferous map, the new thickness maps of the stratigraphic units and detailed stratigraphic information from the new well log interpretations in the study area (Verweij and Witmans, 2009), in combination with regional knowledge and information on paleogeography, sedimentary and structural history (e.g. De Jager, 2007, Geluk, 2007, Van Buggenum and Den Hartog, 2007). Estimated erosional thicknesses were verified with 1D basin modelling at well locations. The following estimated initial thicknesses of stratigraphic units and erosional thicknesses were used in the 3D modelling:

Saalian erosion. This erosion phase affected the Hospital Ground & Step Graben, Maurits, Ruurlo and Baarlo formations (original thicknesses of 400, 200, 400 and 200 m, respectively) with erosion increasing from 150 m in the southwest part of the area to 700 m in the northwest, while deepest erosion occurred in the Hantum Fault Zone area (1000 m).

Mid-Kimmerian erosion. Erosion was concentrated in the Terschelling Basin and on the platforms and highs and affected the Altena and the Upper Germanic Trias groups with maximum values of 600 and 800 m of erosion, respectively. The original thickness of the Altena Group was estimated at 600 m in the Terschelling Basin (present-day thickness = 0 m) and at least 600 m in the Dutch Central Graben (present-day thickness varies between 0 and locally > 1000 m; Figure 8 in Annex 1); the original thickness of the Lower Germanic Trias Group was at least 800 m in the Terschelling Basin (present-day thickness varies between 0 and > 1000 m) and at least 800 m in the Dutch Central Graben (present-day thickness varies between 0 and > 1500 m).

Sub-Hercynian erosion. The scenario for the Cretaceous and Danian sedimentation and erosion history includes the following steps:
The assumed pre-erosional thickness of the Chalk Group is constant (400 m);
The assumed short period of Sub-Hercynian erosion in the Cretaceous is concentrated in the Dutch Central Graben and affects the Chalk and Rijnland groups (maximum erosion 400 and 300 m, respectively);
Deposition of Chalk Group sediments resumes after erosion with thicknesses varying between 0 m in the uplifted eroded centre of the graben to more than 600 m away from the centre.

We created 11 erosion maps (corresponding to the 11 stratigraphic layers affected by erosion) for input into the 3D model (Annex 1). Figure 8 shows an example of a map for the Saalian erosion of the Maurits Formation.
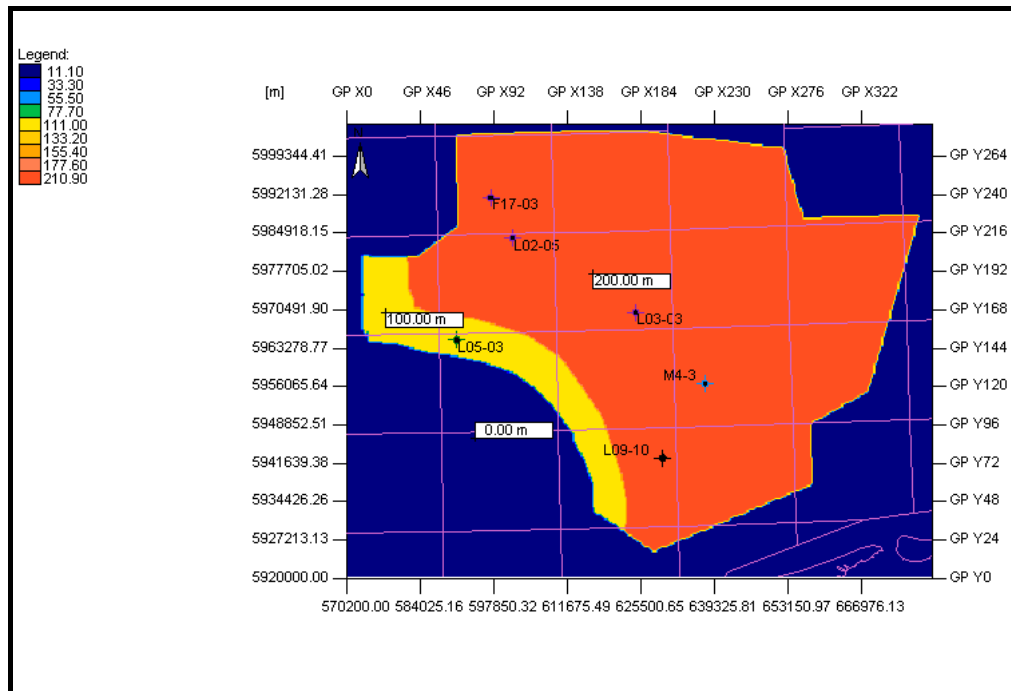
Figure 8. Thickness of the erosion of the Maurits Formation during Saalian phase of erosion.

Paleo water depths. Present-day water depths used in the modelling correspond to
measured water depths. The paleo water depths were allowed to vary in time but were
kept constant over the entire area at a certain time (Figure 9).

Paleo surface temperature. The paleo surface temperature at the sediment water
interface was calculated with an integrated Petromod tool, that takes into account the
paleo water depth and the general evolution of ocean surface temperatures for the
paleolatitude of the area. A correction was applied for present-day temperatures (Figure
9). The temperatures at a certain time are kept constant over the entire area.
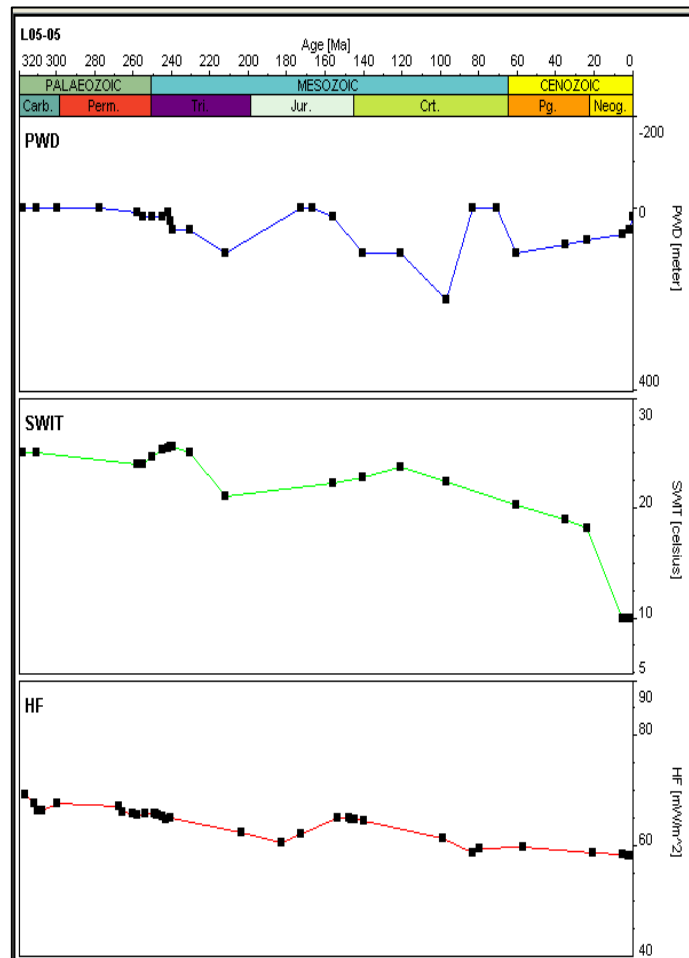
Figure 9. History of water depth (paleo water depth = PWD), sediment water interface temperature (SWIT) and basal heat flow (HF); PWD and SWIT are representative for the whole area; HF shown in this figure is representative for the western part of the area (Dutch Central Graben).

Paleo basal heat flow. Basal heat flow was kept constant at 60 mW/m^2 in the initial 1D-3D Petromod simulations. Later the history of basal heat flow was estimated in-house by applying the 1D tectonic heat flow predicter (Petroprob), using the reconstructed history of sedimentation, uplift and erosion at L05-03 and L09-10 (Abdul Fattah et al. 2008). It was found that the heat flow history in the western and in the eastern part of the area are different due to differences in tectonic subsidence history.

The reconstructed basal heat flow history at the two well locations were used to generate heat flow maps for the whole area for all event times (33 heat flow maps in total). A heat flow map reflects the different basal heat flow histories in the western and eastern part of the area. Figure 9 shows the history of basal heat flow for the western part of the area (Dutch Central Graben).

2.7 Default set-ups, calibration

The Petromod programme provides an extensive suit of default set-ups. Default set-ups that were used in the simulations concern the lithology and mixed lithology and their associated default properties (thermal conductivity, radiogenic heat production, heat capacity), default mechanical compaction equations and default porosity-permeability relations (Annex 2). We selected the Sekiguchi model to calculate the thermal conductivity (Sekiguchi, 1984). The heat capacity is calculated with the Waples model (Waples and Waples, 2004), and Athy's Law is used to derive the mechanical compaction. Measured porosities and permeabilities provided the basis for selecting the proper compaction and porosity-permeability relations. Present-day temperature data and vitrinite reflectance data (Annex 3) were used to calibrate the 1D and later the 3D input model.

3 Modelling results: Burial history and tectonic history

3.1 Burial history

The simulated 1D burial history at wells F17-05 and M01-02 (Figure 6) and the results of the 3D simulated – decompacted – history of sedimentation, uplift and erosion and non deposition (workflow step 3) (Annex 4) revealed a number of interesting features, such as:
There are 3 phases of rapid subsidence and sedimentation that occur in the Dutch Central Graben, Terschelling Basin as well as in the adjacent platform and highs, namely during the Late Carboniferous, Late Permian-Early Triassic (around 270-245 Ma), and Pliocene-Quaternary.
An additional Late Jurassic-Early Cretaceous phase of rapid subsidence and sedimentation (154-140 Ma) is apparent in the Graben and even more so in the Terschelling Basin.

The Saalian phase of uplift and erosion affected the entire area. A second important phase of uplift and erosion in the Mid Jurassic (appr. 173-154 Ma) is limited to the Terschelling Basin and the platform and highs. A third minor phase of uplift and erosion affects the Dutch Central Graben and – especially the western part of – the Terschelling Basin.
Major changes in the geometry of the subsurface, i.e. major changes of the magnitude and dip of the stratigraphic units occur in Jurassic-Early Cretaceous times as a result of the differential subsidence and uplift history of the Dutch Central Graben in comparison with that of the platforms and highs and to a minor extent the Terschelling Basin.

Zechstein salt movement has also significantly affected the sedimentation and erosional history of the basin, and as a consequence the development of the geometry of the area especially since Jurassic times.
The Carboniferous and the Posidonia source rocks are at their maximum depth of burial at present-day.
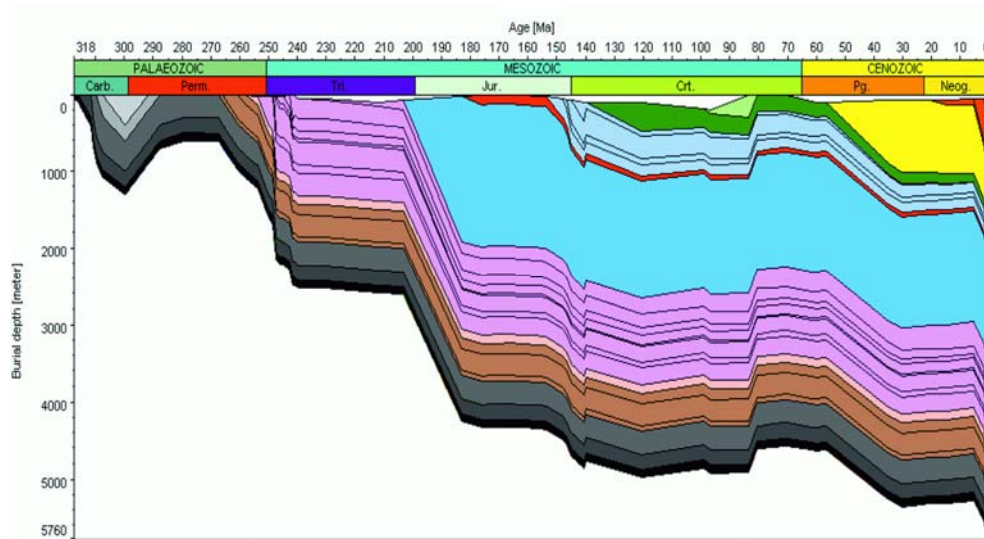
Figure 10a. 1D burial history at well F17-05 in the Dutch Central Graben; note the presence of the complete Altena Group and the Posidonia Shale Formation (red), and the absence of the Chalk Group (light green) due to Late Cretaceous uplift and erosion, and absence of Carboniferous Maurits Formation (light grey) due to Saalian erosion. Movement of Zechstein salt is not included.
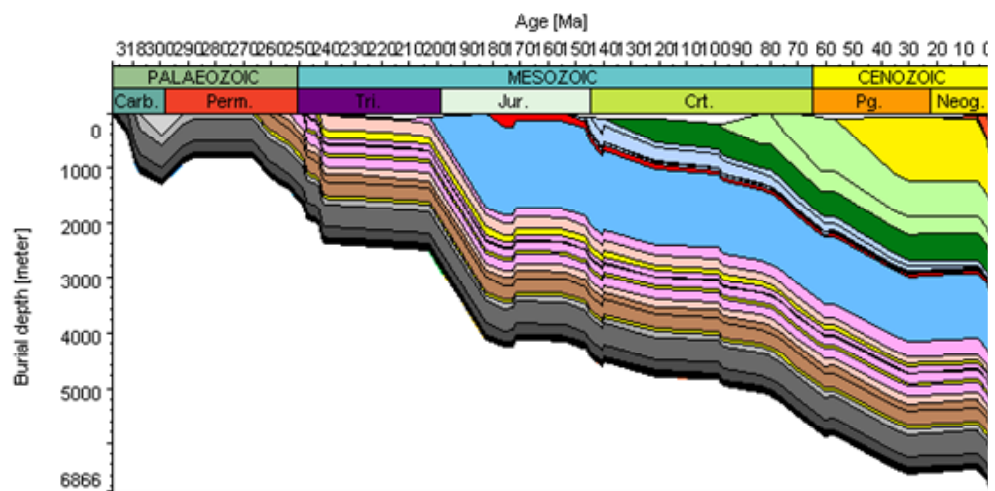

Figure 10b. 1D burial history in block L05 in the Dutch Central Graben; note the presence of the complete Altena Group (blue) and of the Chalk Group (light green), and Carboniferous Maurits Formation (light grey). Movement of Zechstein salt is not included.
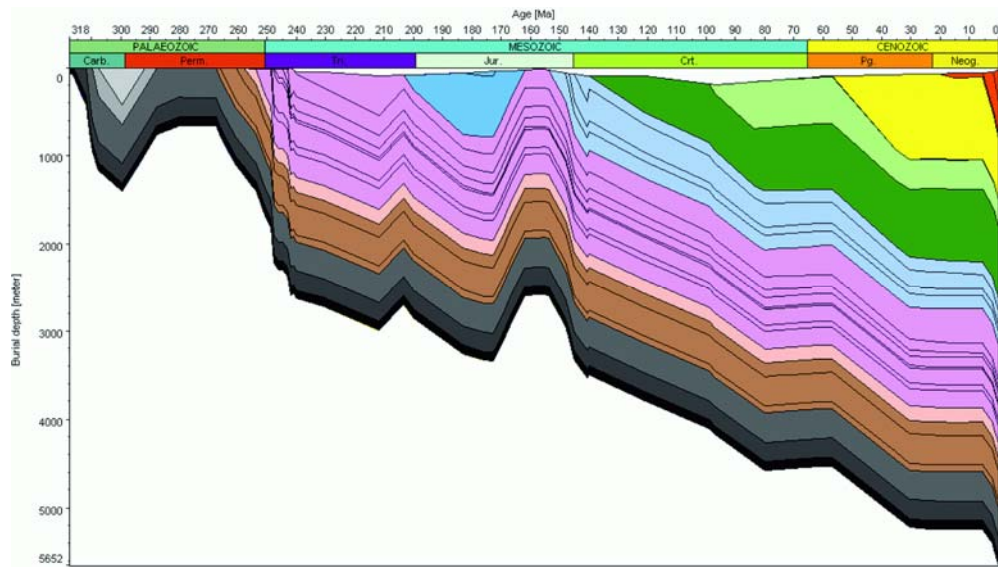
Figure 11. 1D burial history at well M01-02 in the Terschelling Basin; note the complete erosion of the Altena Group during Jurassic uplift and erosion and the absence of the Posidonia Shale Formation. Movement of Zechstein salt is not included.

3.2   Tectonic subsidence

The tectonic subsidence was reconstructed by Abdul Fattah et al. (2008) at 6 well locations using probabilistic tectonic heat flow modelling (Van Wees et al., 2009): F17-03, L02-05 and L05-03 in the Dutch Central Graben, M04-03 and L03-03 in the Terschelling Basin and L09-10 on the Vlieland High. The reconstruction was based on the same time sequence of events, lithologies and PWD and SWITs used for the Petromod simulations, while important lithology-dependent compaction and thermal parameters were made consistent as much as possible with the default parameter values incorporated in Petromod. Tectonic subsidence is calculated from the decompacted burial history at the wells. This involves removing the impact of decompacted sediments, isostatic balancing and the paleo water depth from the subsidence curve of the well. The resulting tectonic subsidence is called the observed tectonic subsidence as it is obtained from the observed thicknesses and lithology parameters of the formations.
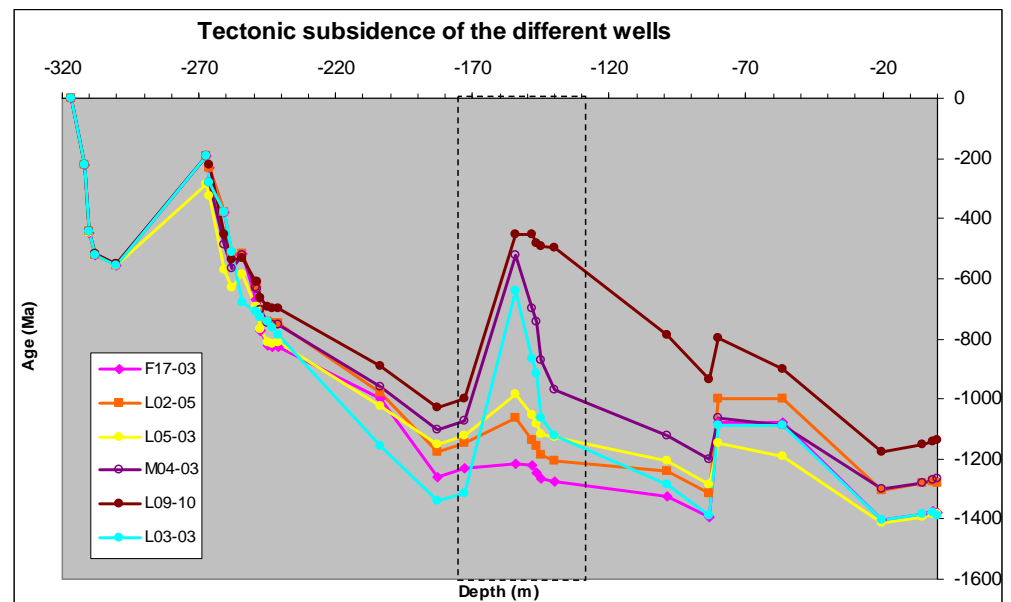

Figure 12. Tectonic subsidence at 6 well locations. Note the difference in amount of uplift around 160 Ma between the wells F17-03, L02-05, L05-03 located in the Dutch Central Graben and the wells M04-03, L03-03, L09-10 located in the Terschelling basin and on the Vlieland High (L09-10) (From Abdul Fattah et al. 2008).

The observed tectonic subsidence history (Figure 12) reveals two phases of rapid subsidence at all well locations, namely during the Late Carboniferous and Late Permian-Early Triassic (around 270-245 Ma). In addition, Figure 12 shows a Late Jurassic-Early Cretaceous phase of rapid tectonic subsidence in the Terschelling Basin that was also apparent in the burial history of the basin. The 3rd phase of rapid subsidence in Pliocene-Quaternary times observed in the burial histories of the whole area (Figures 10 and 11) does not appear in the tectonic subsidence reconstruction.

The main regional difference in tectonic subsidence history concerns the amount of uplift around 160 Ma between the wells F17-03, L02-05, L05-03 located in the Dutch Central Graben and the wells M04-03, L03-03, L09-10 located in the Terschelling Basin and on the Vlieland High (L09-10). Abdul Fattah et al. (2008) performed forward modelling of the tectonic subsidence at two well locations (L05-03 and L09-10) representing the two different tectonic histories. The McKenzie model was used for the forward tectonic modelling, except during the Jurassic uplift phase which was defined as an underplating event, i.e. a thermal phase of thermal uplift.

Figures 13 and 14 show the best fitting tectonic subsidence and the associated crustal stretching factors (d). The crustal stretching factors for the Saalian and the late Cretaceous uplift phases are less than 1, indicating that the crust undergoes shortening as a result of tectonic inversion. The crustal stretching factor for the Mid-Late Jurassic uplift phase d=1 (and a subcrustal stretching b>1), reflects the fact that uplift was set to be caused by thermal uplift and mantle upwelling rather than tectonic inversion (Abdul Fattah et al. 2008).
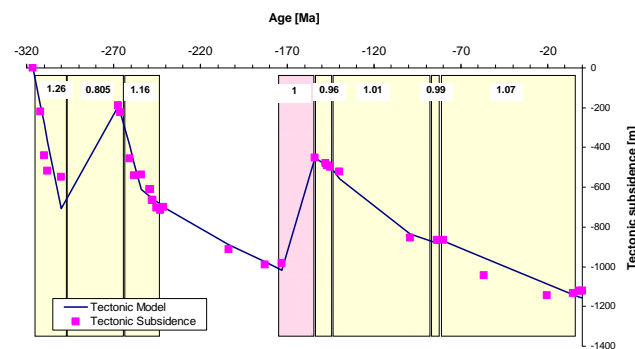

Figure13.   Modelled tectonic subsidence with associated crustal stretching factors and observed tectonic subsidence at well L09-10 (Terschelling Basin/Vlieland High) (Abdul Fattah et al. 2008).
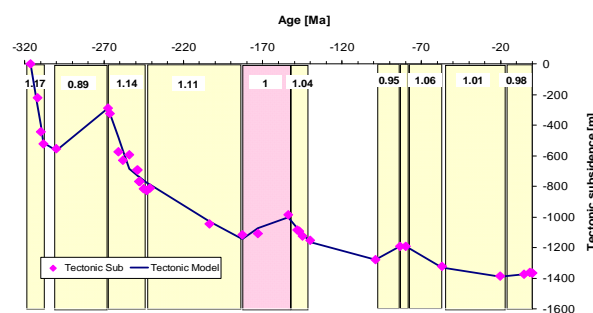

Figure 14. Modelled tectonic subsidence with associated crustal stretching factors and observed tectonic subsidence at well L05-03 (Dutch Central Graben) (from Abdul Fattah et al. 2008).

4   Modelling results: Temperature and heat flow history

The simulations of the temperature and heat flow history started with a thermal model, applying default Petromod lithology-related thermal conductivities (Sekiguchi model), heat capacities and radiogenic heat production, and a constant basal heat flow of 60 mW/m^2 as bottom boundary condition, zero heat flow across lateral boundaries, a transient heat flow through the sediments, and the history of sediment water interface temperatures. Note that Petromod simulations do not take the influence of fluid flow on thermal conditions in the basin into account.

Present-day temperatures and vitrinite reflectance measurements were available for calibration purposes.

A second scenario for the thermal modelling incorporated the results of a tectonic reconstruction of the basal heat flow boundary condition (section 4.1 and 4.2)

4.1   Basal heat flow history

The history of basal heat flow was reconstructed by Abdul Fattah et al. (2008), using Petroprob and the burial histories of wells L05-03 and L09-10, representative for the western area (Dutch Central Graben) and the eastern area (Terschelling Basin and Vlieland High), respectively. The reconstructed tectonic subsidence and associated heat flow are shown in Figures 15 and 16.
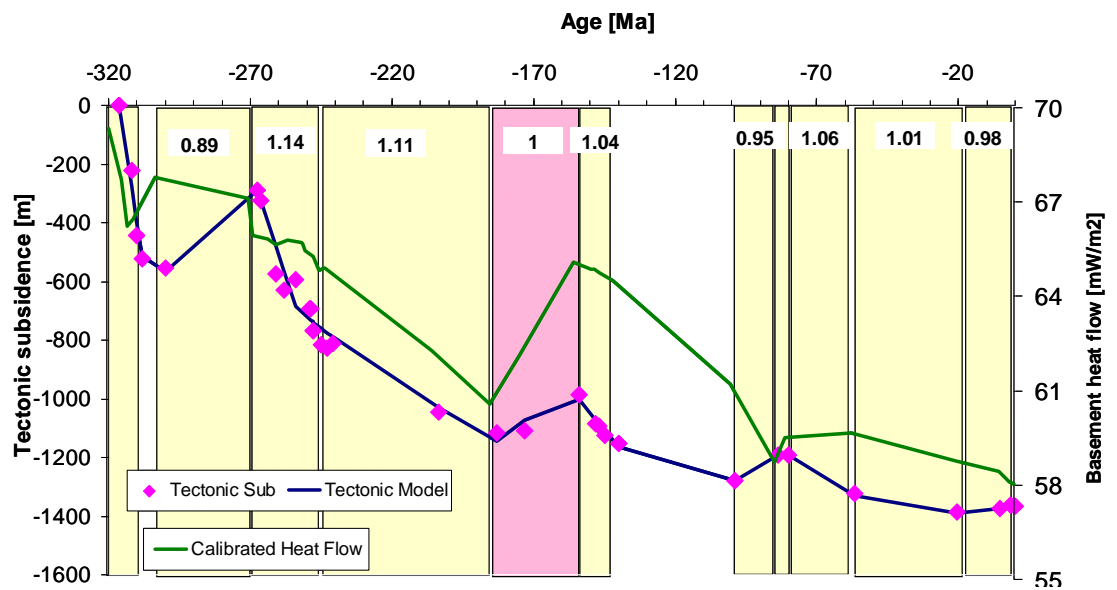

Figure 15. Calibrated basal heat flow and tectonic subsidence at well L05-03 (Dutch Central Graben) (from Abdul Fattah et al. 2008).
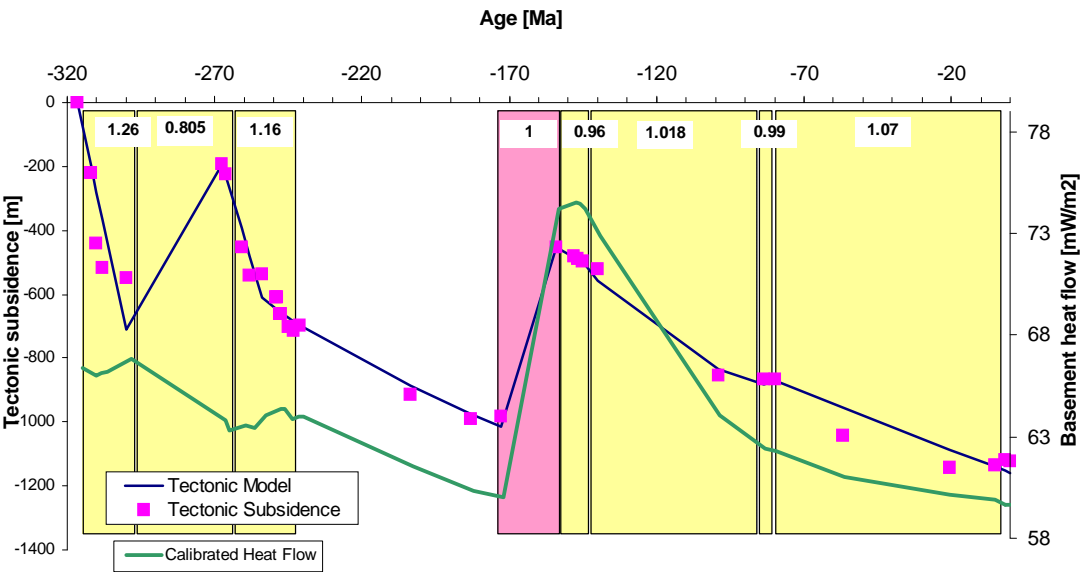
Figure 16. Calibrated basal heat flow and tectonic subsidence at well L09-10 (Terschelling Basin/Vlieland High) (from Abdul Fattah et al. 2008).

Modelling results indicate that present day basal heat flow at both wells is at its minimum, reaching values of 58 - 60 mW/m^2 with the slightly higher values in the eastern part of the area. The Mid-Late Jurassic uplift is associated with a peak in basal heat flow reaching values of 77mW/m^2 in L09-10 and 65mW/m^2 in L05-03 (Dutch Central Graben). These reconstructed basal heat flow histories were used to generate heat flow maps imported as boundary conditions for the 3D Petromod basin modelling (Figure 17).
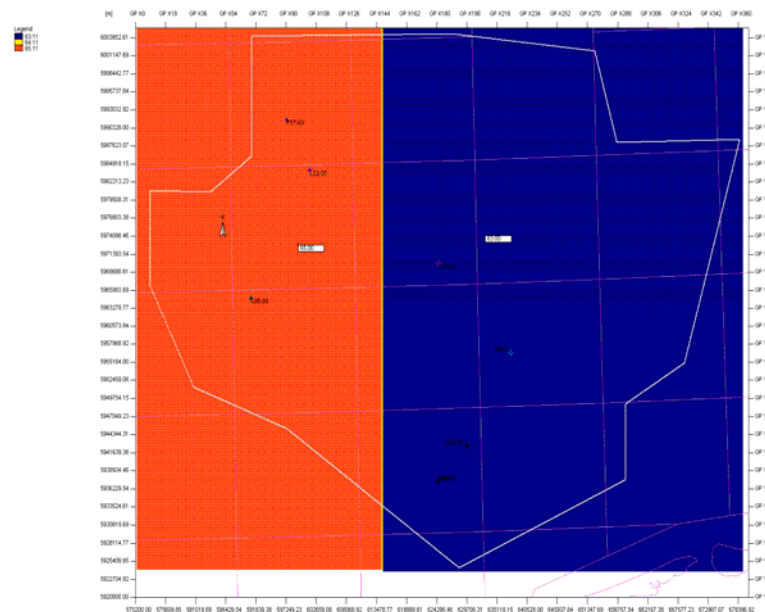

Figure 17. Example of basal heat flow map at 245 Ma. The map is based on extrapolation of heat flow values obtained at well locations, representative for the western part of the area (well L05-03; heat flow=65 mW/m^2 at 245 Ma; red area) and eastern part (well L09-10; heat flow = 63 mW/m^2 at 245 Ma; blue area), respectively.

The variable basal heat flow boundary condition reconstructed from tectonic forward modelling produces a generally higher heat flow input during history in comparison with the constant boundary condition of 60 mW/m^2 (Figure 18).

The evaluation of the influence of these two different boundary conditions on the 1D and 3D simulation of temperature and maturity history indicated that there are no to only very slight differences in simulated present-day temperature and vitrinite reflectance values and that the simulation results are in accordance with measured temperature and vitrinite reflectance data (Figure 19). Figure 19 shows that there is a difference between the results of the 1D and 3D simulations: the 3D simulations result in lower present-day temperatures and vitrinite reflectance values, especially at greater depths. This difference has no relation with the different basal boundary conditions, but is largely due to the unrealistic overpressure effect on temperature and heat flow in the 1D modelling (Verweij, 2007).

The two different thermal boundary condictions result in different evolutions of temperature and maturity with time. The main differences in simulated temperature occur from the Mid-Jurassic to the end of the Cretaceous and the differences in maturity appear with a time-delay from the Early Cretaceous to the Early Paleogene (Figure 18); temperatures and maturities reach higher values for the variable basal heat flow boundary condition. However, these differences disappear again during the Paleogene. The evaluation suggests that the Mid-Late Jurassic peak in basal heat flow influences the timing of maturation but not the maximum maturity level of the source rock reached during its geologic history in the studied area.
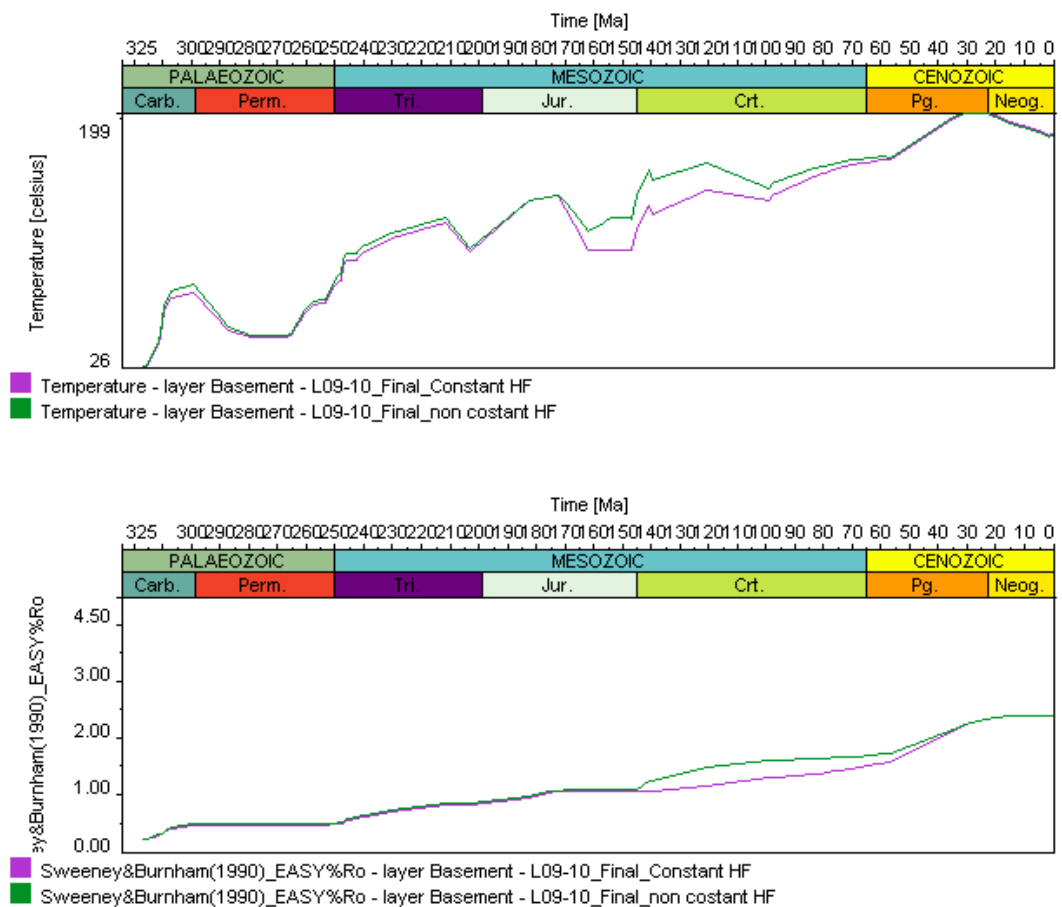

Figure 18.   Simulated temperature and heat flow history for the deepest layer in well L09-10 for constant heat flow boundary condition of 60 mW/m² (purple line) and for variable heat flow boundary condition (green line).
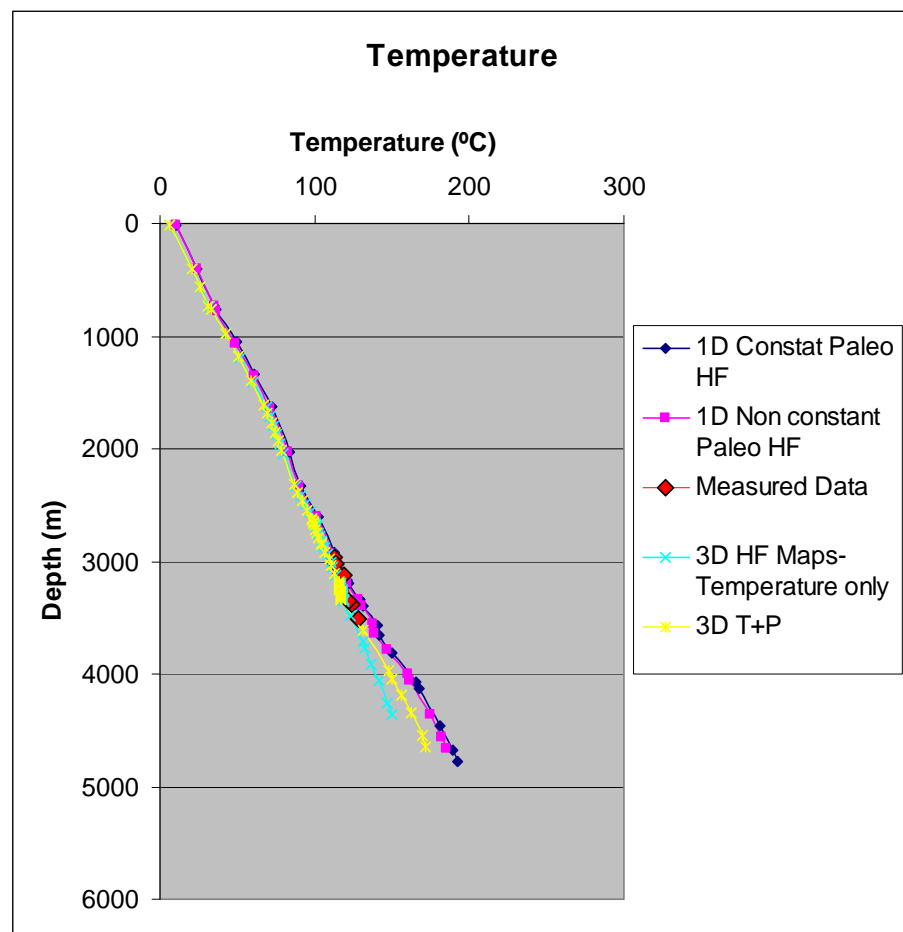
Figure 19. Present-day temperatures resulting from 1D simulations of temperature history at well L09-10, using constant and variable basal heat flow boundary conditions (dark blue: constant basal heat flow = 60 mW/m^2; pink: variable basal heat flow). Present-day temperatures resulting from 3D simulations of temperature history at well L09-10 using a variable basal heat flow boundary condition for hydrostatic conditions (light blue) and hydrodynamic conditions (yellow). The 1D and the hydrodynamic 3D simulations include overpressured and undercompacted conditions at greater depths resulting in higher present-day temperatures at greater depths.

In conclusion, the incorporation of the time-dependent changes in basal heat flow into the boundary conditions resulted in higher calculated paleo temperatures and paleo maturities (vitrinite reflectance values), especially in the deeper parts of the basin, during the periods of 'underplating' related increased basal heat flow. The temperatures are clearly different in the preiod 170 - 55 Ma, while the maturities deviate between approximately 145 – 35 Ma.

4.2   Temperature history

The 3D temperature history is reconstructed using the tectonic heat flow boundary condition, in combination with the sediment water interface temperatures and paleo water depths given in Figure 9. Annex 5 includes examples of calibration results for 1D extractions at well locations of 3D temperature simulations.

The temperature distribution in a sedimentary basin at a certain time during history, assuming steady state conditions, principally depends on the the spatial variation in basal heat flow input, the distribution of bulk thermal conductivities of the subsurface and the sediment water interface temperatures. Bulk thermal conductivities of clastic lithostratigraphic units and carbonates broadly range between values of 1.5 and 3.5 $Wm^{-1}K^{-1}$. The bulk thermal conductivities of halites and anhydrites vary between approximately 2.8 and 5 $Wm^{-1}K^{-1}$. Because the thermal conductivities of salt decreases as a function of increasing temperature, and therefore depth, the deeper salt units tend to act thermally similarly to other sediments.

However, within the shallower part of a basin, salt diapiric structures can significantly disturb heat flow. Focussing of heat flow through salt structures will increase temperatures in the top part of the salt structures and in adjacent lithostratigraphic units, while decreasing the temperatures in units immediately underlying the salt structures. Figure 20 shows simulation results of the 3D modelling and clearly illustrates the 3D effect of the salt structures on the temperature and heat flow distribution (and as a consequence on source rock maturity values).
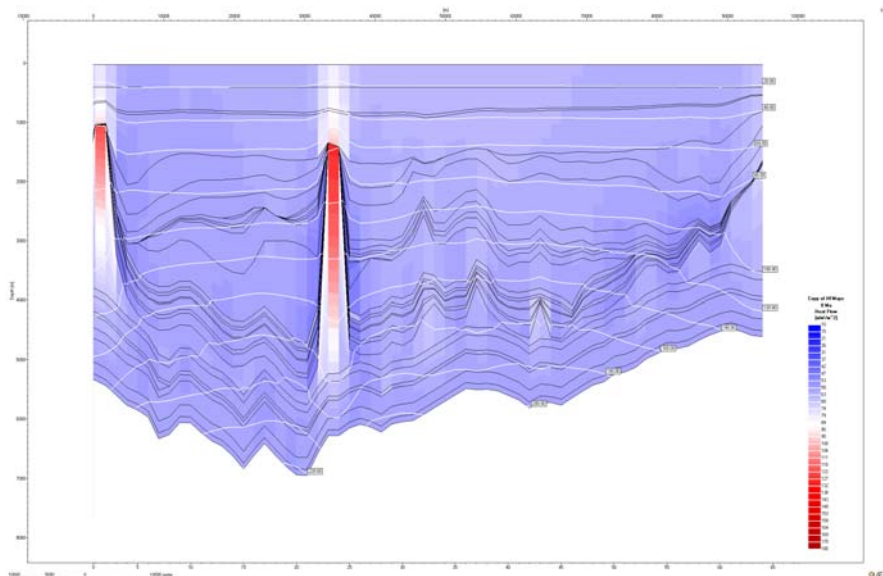

Figure 20. Influence of salt structures on present-day temperature and heat flow distribution (2D W-E extraction of 3D simulation results; same cross section as shown in Figure 7). High heat flowws through salt structures (in red) are associated with increased temperatures in sediments close to the top of the salt structure and reduced temperatures below salt structures. The reduction of temperatures below the salt structures also affects the Carboniferous source rocks.

Annex 6 presents the simulated present-day temperature distribution in map view at different depths. These maps reveal large regional variations in temperature of more than 20°C at each depth and clearly illustrate the effect of salt structures on the temperature distribution. These observations confirm previous analysis of measured present-day temperatures (Verweij and Witmans, 2009).

For steady state Petromod simulations the regional variations in temperature in a stratigraphic unit at a certain time in history mainly result from regional variation of: depth of burial, basal heat flow, and bulk thermal conductivity sedimentary sequence. Transient simulations incorporate effects of paleo boundary conditions (e.g. paleo surface temperatures) and effects of rapid sedimentation or uplift on the temperature distribution at a certain time.

Representative results of transient 3D simulations of temperature evolution of the source rock units (Posidonia Shale Formation, and the Maurits, Ruurlo and Baarlo formations), using the variable basal heat flow boundary condition, are summarised below.

4.2.1   Calculated thermal evolution of the Posidonia Shale Formation

The distribution area of the Posidonia Shale Formation was greatly reduced by erosion shortly after its deposition in Jurassic times. In the stidy area, erosional remnants occur in the Dutch Central Graben only (Figure 21).
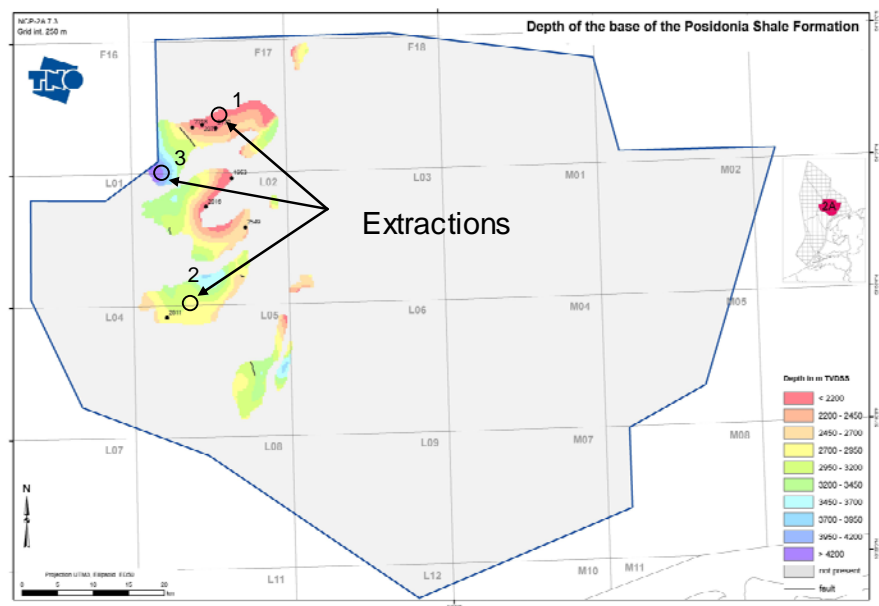

Figure 21. Present-day distribution and depth of the Posidonia Shale Formation in the southern part of the Dutch Central Graben. Locations of the selected 1D extractions of the 3D simulation of burial, temperature and maturity history of the Posidonia Shale Formation: Location 1. block F17 (present-day depth Posidonia = 1745 m); Location 2. block L02 (present-day depth Posidonia = 2762 m); Location 3. SW part of block 17 (present-day depth Posidonia =3768 m).

The time-dependent basal heat flow input for the 3D Petromod modelling is constant at a certain time for the whole Dutch Central Graben. As a consequence, simulated regional variations in calculated temperature history of the Posidonia will result mainly from differences in burial history, and more locally from differences in position relative to salt structures. The burial history of the Posidonia shows large differences (Figures 21 and 22) resulting in very different temperature histories depending on its structural position (Figure 23). The burial history and related temperature histories at three locations are shown in Figures 22 and 23, respectively.

Location 1 (block F17; present-day depth Posidonia = 1745 m). Only minor burial of the Posidonia until the Late Cretaceous uplift and erosion results in pre-uplift temperature of only 65°C. Subsidence in the Paleogene increases the temperature to a maximum value of 80°C at the end of the Paleogene.
Location 2 (block L02; present-day depth Posidonia = 2762 m). This location is outside the area that was seriously affected by Late Cretaceous uplift and erosion. The Posidonia subsides continuously until the end of the Paleogene and reaches a maximum temperature of 120°C.
Location 3 (southwestern part of block F17; present-day depth Posidonia = 3768 m). Burial history is characterised by rapid and deep burial during the Late Jurassic and continued burial until the Late Cretaceous uplift and erosion, followed by resumption of burial during the Paleogene. Temperatures reach values of 120°C before Late Cretaceous erosion, and maximum source rock temperatures are reached in the Late Paleogene = 150°C.

During the Latest Paleogene and subsequent Neogene times the temperatures in the source rock decrease also during times of increasing burial probably due to the sharply decreasing sediment water interface temperatures (Figures 22 and 23) in combination with the relatively low basal heat flow. Only very recently, the temperatures in the source rock start to increase again. Present-day temperatures in the Posidonia Shale Formation are less than previous values.
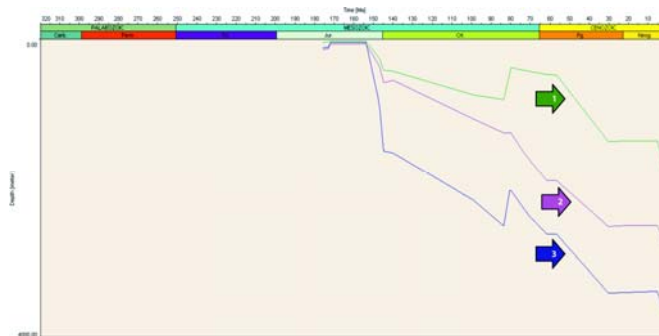

Figure 22.   Simulated burial history of the Posidonia Shale Formation at the three selected locations 1. block F17; 2. block L02; 3. SW part of block 17 (see Figure 21 for location).
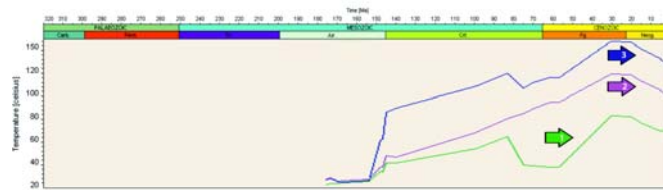
Figure 23. Simulated temperature history of the Posidonia Shale Formation at the three selected locations 1. block F17; 2. block L02; 3. SW part of block 17 (see Figure 21 for location). Maximum temperatures were reached at the end of the Paleogene.

4.2.2   *Calculated thermal evolution of the Carboniferous source rocks*
The Carboniferous source rocks Baarlo and Ruurlo Formations are present throughout the area, in both the Dutch Central Graben and the Terschelling Basin (Figure 24).
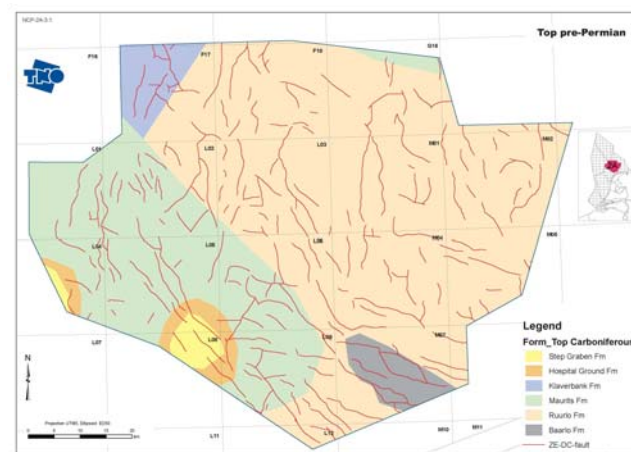

Figure 24. Top Carboniferous at present-day.

Lateral variations in calculated temperature history of these source rocks will mainly result from differences in burial history, position relative to salt structures, and – in contrast to the Posidonia Shale Formation – also from differences in basal heat flow history between the western and eastern part of the study area.

Results from four representative 1D extractions of 3D simulations of burial and temperature history in the Ruurlo Formation (Figures 25) illustrate the temperature evolution in the Carboniferous source rocks in the Dutch Central Graben, Terschelling Basin and Vlieland High (Figure 26).
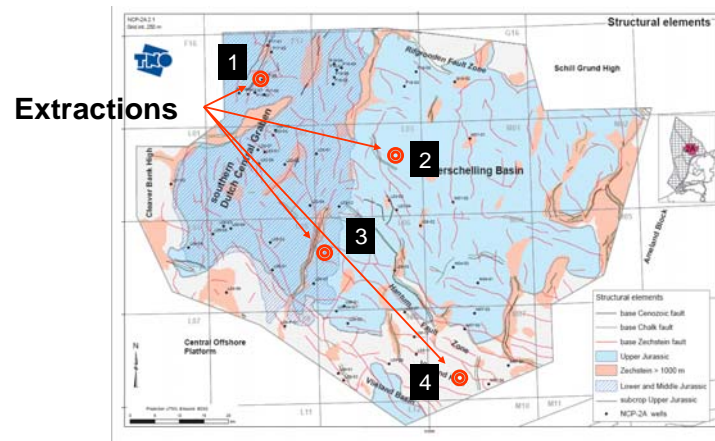
Figure 25. Four selected 1D extractions of the 3D simulation of burial, temperature and maturity history of the Carboniferous source rocks: location 1: block F17 in the Dutch Central Graben; locations 2 and 3: blocks L03 and L06 in the Terschelling Basin; location 4: block M07 on Vlieland High.
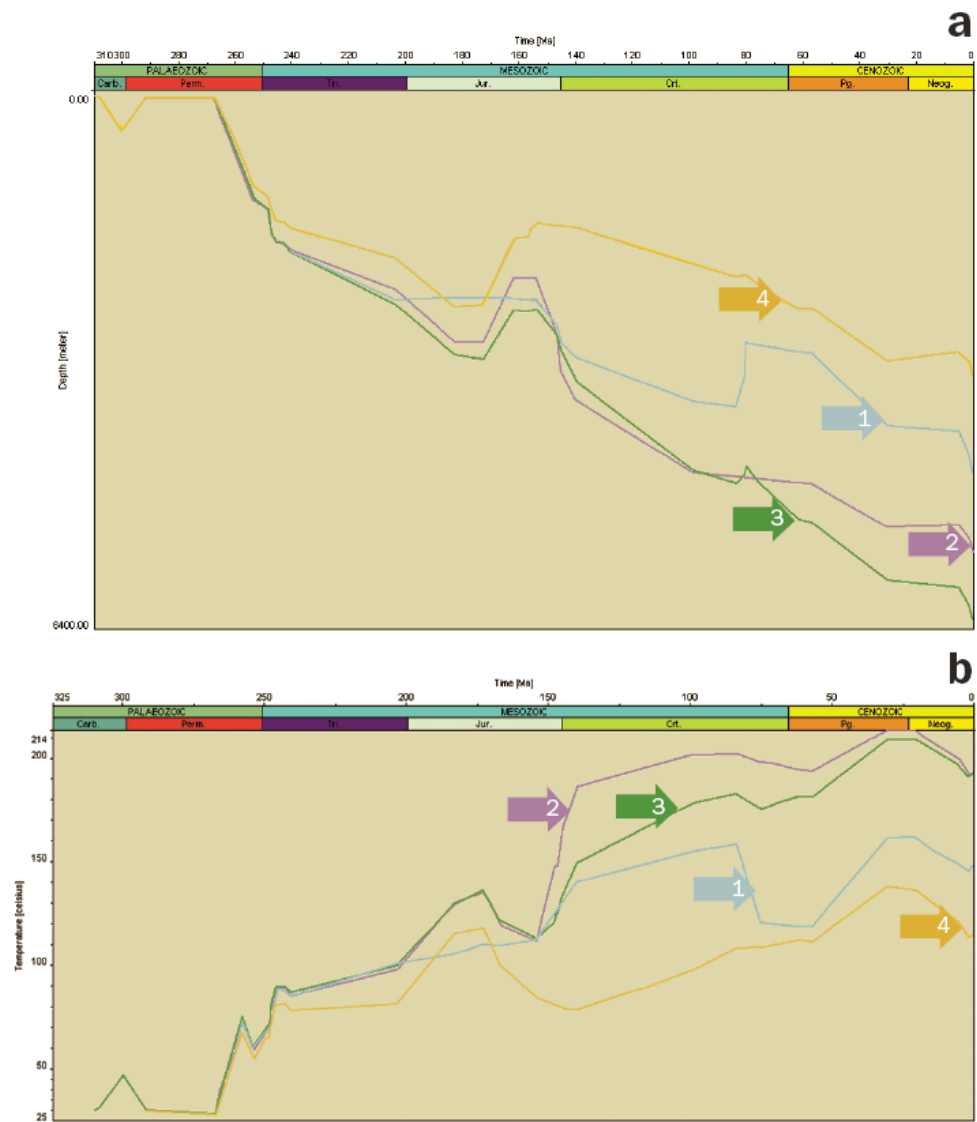
*Figure 26 **a**. Selected 1D extractions of the 3D simulation of burial history of the Ruurlo Formation. At present-day the Ruurlo Formation is at maximum burial depth at all 4 locations. **b**. Selected 1D extractions of the 3D simulation of temperature history of the Ruurlo Formation. Maximum temperatures of the Ruurlo Formation are reached at Late Paleogene times. Location 1: block F17 in Dutch Central Graben (blue); locations 2 and 3: blocks L03 and L06 in the Terschelling Basin (purple and green, respectively); location 4: block M07 on Vlieland High (yellow) (see Figure 25 for location of the 1D extractions).*

Maximum temperatures are reached in Late Paleogene times, and all present-day temperatures are less than the previous Late Paleogene temperatures at all four locations.

The broadly similar burial histories of the Carboniferous source rocks in the Terschelling Basin (blocks L03 and L06) and Vlieland High (block M07) until the Mid-Late Jurassic uplift and erosion phase leads to pre-uplift temperatures of the Ruurlo source rocks of 135 and 120°C, respectively. In the Terschelling Basin these Jurassic pre-uplift temperatures are exceeded again around the Jurassic-Cretaceous boundary and increases to values of 180-200°C until the Late Cretaceous uplift period. In contrast, the Jurassic pre-uplift temperatures on the Vlieland High (block M07) are not exceeded unitil Paleogene times. The temperatures of the Ruurlo Formation in the Dutch Central Graben (block F17) increase continuously from Late Permian until the Late Cretaceous uplift of the graben and reaches values of 160°C. This temperature is hardly exceeded during the post-uplift times.

In conclusion, the temperature history at the four locations largely follows the burial histories of the source rocks. The temperatures in the source rocks increase with increasing depth of burial and decrease during uplift and erosion. Uplift and erosion in the Mid-Late Jurassic in Terschelling Basin and Vlieland High is associated with decreasing temperatures in spite of the contemporaneous increasing basal heat flow. Post-uplift burial in combination with the relatively high basal heat flow result in rapidly increasing temperatures in the Terschelling Basin and to a minor extent in the Dutch Central Graben.

The temperatures of the Carboniferous source rocks decrease from Late Paleogene to Pliocene times, also during times of increasing burial. Only very recently, temperatures start to increase again. The decreasing temperatures in the source rocks probably largely result from the significant decrease in surface temperatures from Late Paleogene onward (Figure 9). The simulated present-day temperatures in the Carboniferous source rocks are lower than the maximum temperatures experienced during previous burial.

5 Modelling results: History of maturity and hydrocarbon generation

Petromod calculates maturity indicators such as vitrinite reflectance values (according to Sweeney and Burnham 1990) and transformation ratios. Vitrinite reflectance values are calculated for all stratigraphic units. The transformation ratio is the ratio of generated petroleum to potential petroleum in a source rock. The transformation ratio provides information on the timing of hydrocarbon generation and is calculated for the source rock units. The calculation of the transformation ratios are based on the Burnham (1989)_T2 kinetic model for the Posidonia Shale Formation and the Burnham (1989)_T3 kinetic model for the Carboniferous source rocks.

5.1 History of maturity and hydrocarbon generation of the Posidonia Shale Formation

The different burial and temperature histories of the Posidonia Shale Formation in the Dutch Central Graben (Figures 22 and 23) resulted in associated different maturity histories (Figure 27). The calculated transformation ratios (Figure 28) indicate that in the southwestern part of block F17 the Posidonia Shale Formation already starts generating hydrocarbons in Cretaceous times with generation rates reaching their maximum values just before Late Cretaceous uplift. The generation is resumed in Paleogene times and practically stops at the end of the Paleogene. At location 2 (block L02) the maturity of the Posidonia increases gradually and the source rock starts generating hydrocarbons not until the Paleogene and continues into the Neogene. In the inverted centre of the Dutch Central Graben (location 1) the Posidonia did not reach a mature state for hydrocarbon generation (Vr< 0.55; Figure 28).
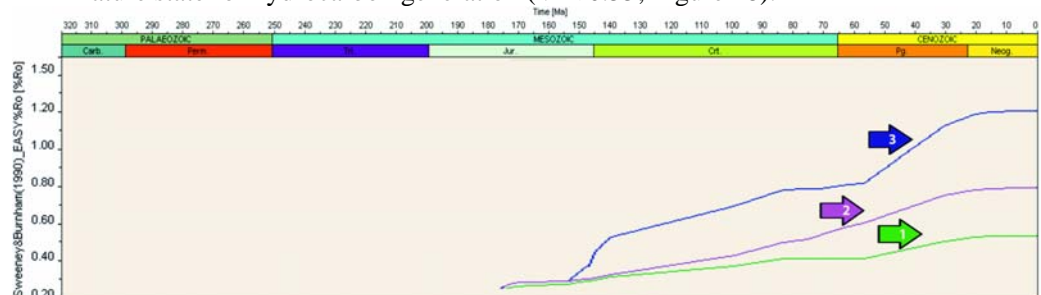

Figure 27 Simulated maturity history of the Posidonia Shale Formation at the three selected locations 1. block F17; 2. block L02; 3. SW part of block 17 (see Figure 21 for location).
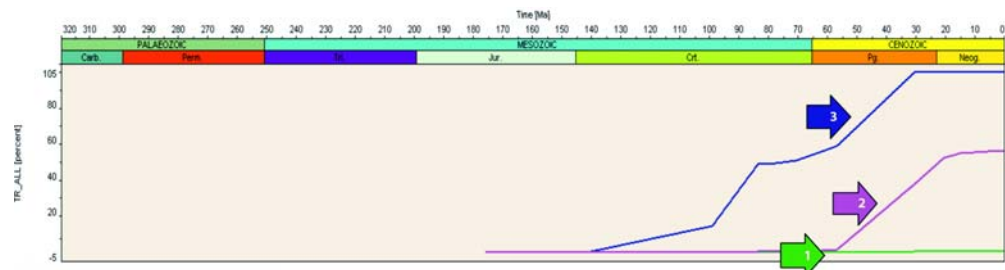

Figure 28 Simulated history of transformation ratios for the Posidonia Shale Formation at the three selected locations 1. block F17; 2. block L02; 3. SW part of block 17 (see Figure 21 for location).

5.2   History of maturation and hydrocarbon generation in Carboniferous source rocks

The simulated histories of maturity and transformation ratios for the Ruurlo and Baarlo formations in the graben and the Terschelling Basin reveal important information on the timing of hydrocarbon generation (Figures 29 and 30). The calculated transformation ratios reveal a first phase of hydrocarbon generation before the Mid-Kimmerian uplift in the Terschelling Basin (Figure 30). A major phase of hydrocarbon generation is apparent in Latest Jurassic and Early Cretaceous times in both the Graben and the Basin. There is only limited resumption of hydrocarbon generation in the Graben and a variable resumption of hydrocarbon generation in the Terschelling Basin during Paleogene times, after the Sub-Hercynian uplift. Top view maps of the maturity distribution of the Ruurlo Formation before and after Sub-Hercynian uplift (Figures 31 and 32) show a clear increase of source rock maturity along the boundaries of the study area. This is indicative of a Tertiary phase of hydrocarbon generation from Carboniferous source rocks on the Cleaver Bank High, Central Offshore Platform, Vlieland High and Schill Grund High.
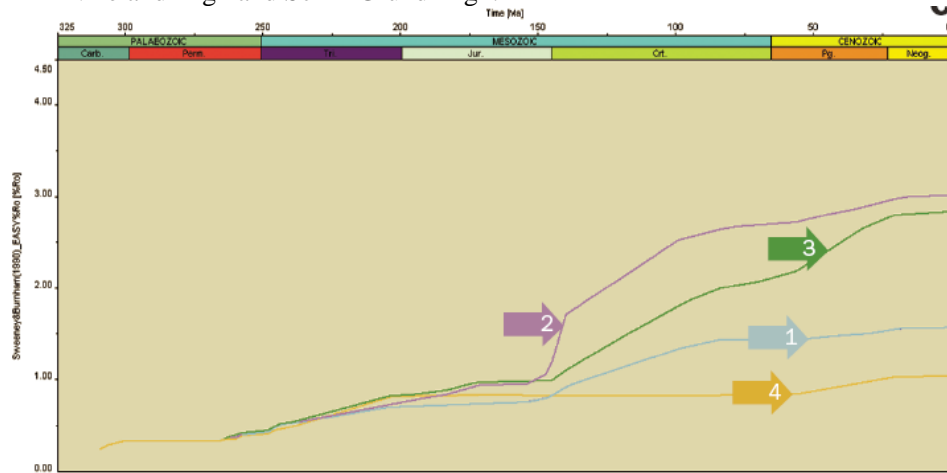

Figure 29.   Selected 1D extractions of the 3D simulation of maturity history of the Ruurlo Formation. Location 1: block F17 in Dutch Central Graben; locations 2 and 3: blocks L03 and L06 in the Terschelling Basin; location 4: block M07 on Vlieland High (see Figure 25 for location 1D extractions).
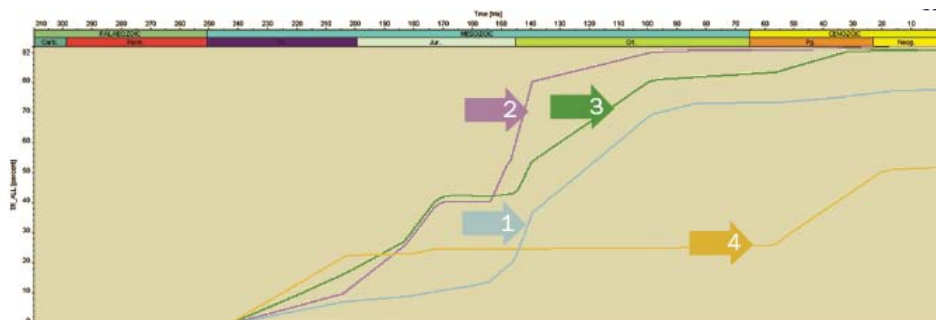

Figure 30. Simulated history of transformation ratios for the Ruurlo Formation. . Location 1: block F17 in Dutch Central Graben; locations 2 and 3: blocks L03 and L06 in the Terschelling Basin; location 4: block M07 on Vlieland High High (see Figure 25 for location 1D extractions).
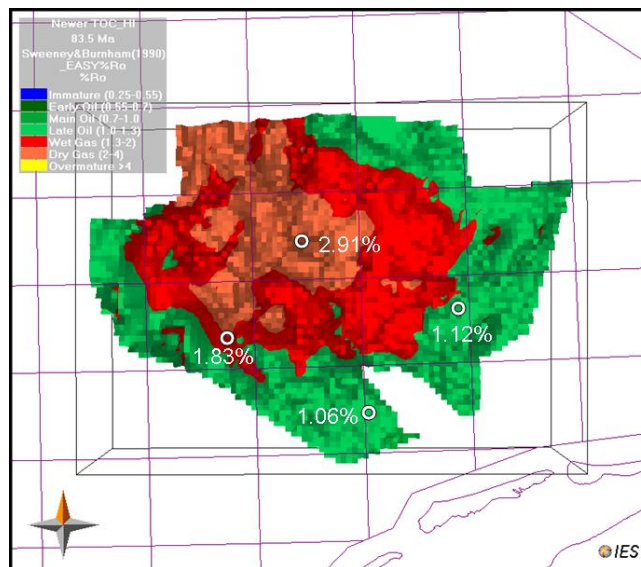
Figure 31. Top view: distribution of calculated maturity (vitrinite reflectance values) at the top of the Ruurlo Formation just before Sub-Hercynian uplift (83.5 Ma).
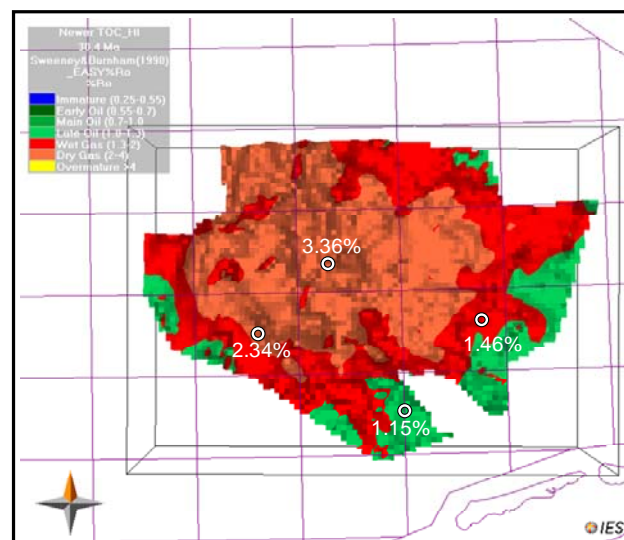

Figure 32. Top view: distribution of calculated maturity (vitrinite reflectance values) at the top of the Ruurlo Formation after Sub-Hercynian uplift (30.4 Ma).

5.3   Present-day maturity

Present-day vitrinite reflectance values for the Posidonia Shale Formation and the Carboniferous source rocks were extracted from the 3D simulation of the geological model (Vr calculations based on Sweeney and Burnham 1990) and are shown in Figure 33. This figure shows that present-day vitrinite reflectance values of the Posidonia Shale Formation vary widely from immature to wet gas conditions. In large part the maturity increases with present-day depth of burial (Figure 33).
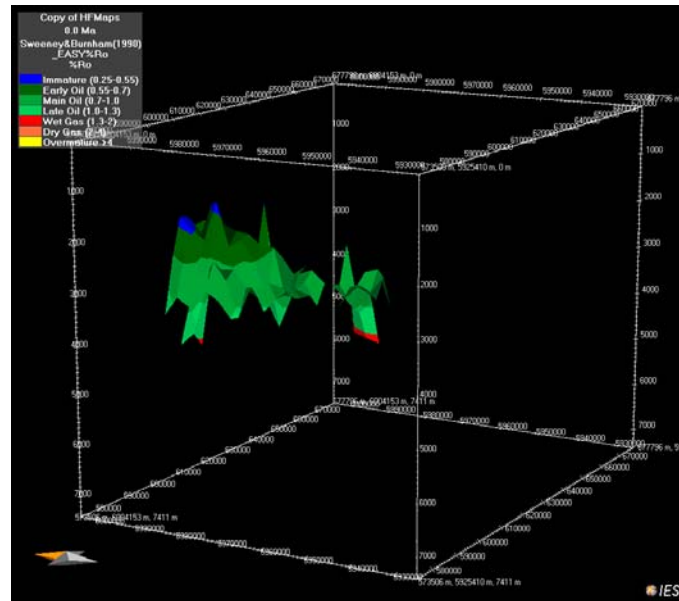

Figure 33.   Distribution of calculated vitrinite reflectance values for the Posidonia Shale Formation at present-day. The range of vitrinite reflectance values represents immature to wet gas conditions (orange arrow points to the north).

The calculated present-day variation of maturity at the top of the Maurits and Ruurlo formations shows that these source rocks are in the dry gas window in large parts of the Graben and Basin (Figures 34 and 35). The above described cooling effect of large salt structures on temperatures in the sub-salt stratigraphic units (Figure 20, Annex 6) also influenced the maturity history of these sub-salt source rocks. Figure 36 illustrates that local wet gas conditions in the Graben and Basin are related to salt structures. The relatively shallow burial depth of the Carboniferous source rocks along the borders of Central Graben and the Terschelling Basin and on the adjacent platform and highs during the large part of geological history (Figure 26) is reflected in the wet gas conditions (Figures 34 and 35).
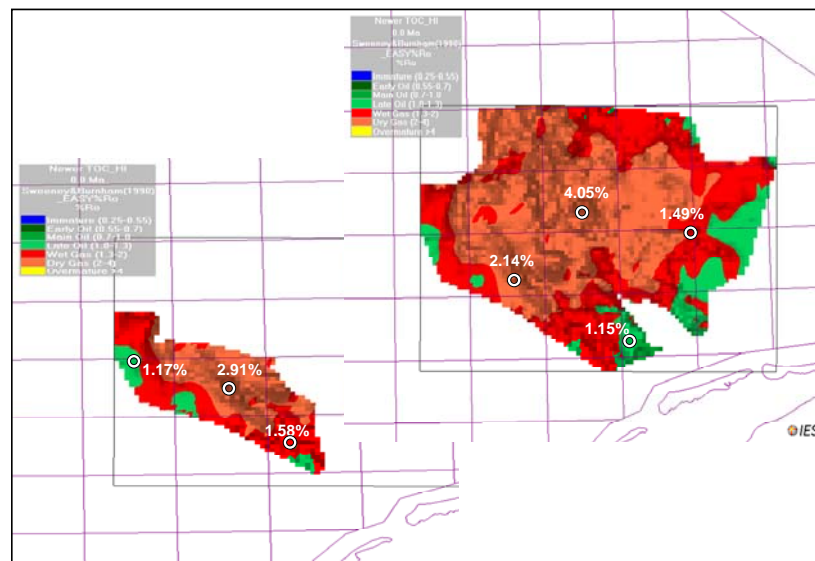
Figure 34. Top view: distribution of calculated present-day maturity (vitrinite reflectance values) at the top of the Maurits Formation and the Ruurlo Formation (left and right-hand side of figure, respectively). Maturity of Ruurlo Formation varies between overmature (> 4%Ro) in the deepest part of the Terschelling Basin to immature for gas generation (green) in the platform and highs adjacent to the Terschelling Basin and the Dutch Central Graben (according to Sweeney and Burnham 1990 maturity classification).
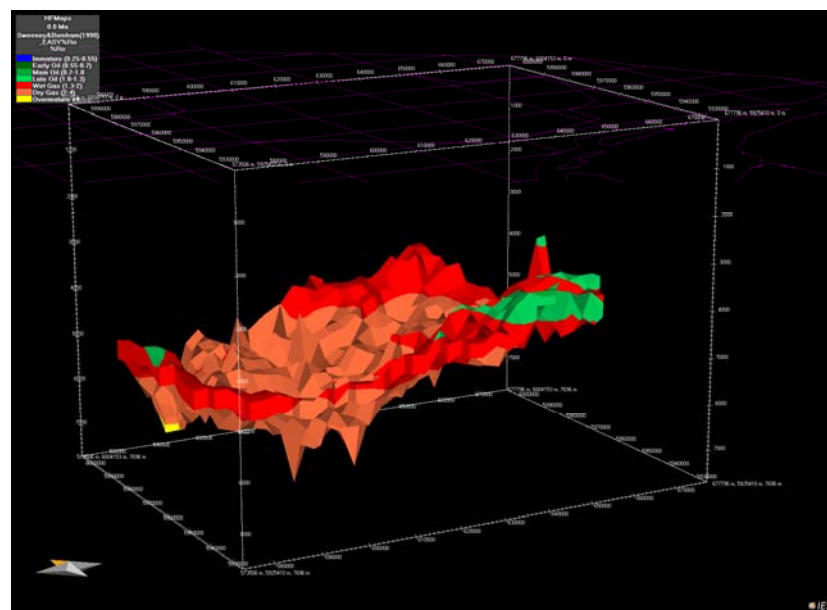

Figure 35. Lateral view (orange arrow points to the north): distribution of calculated present-day maturity (vitrinite reflectance values) of the Ruurlo Formation. Maturity of the Ruurlo Formation varies between overmature (yellow) in the deepest part of the Central Graben to immature for gas generation (green).
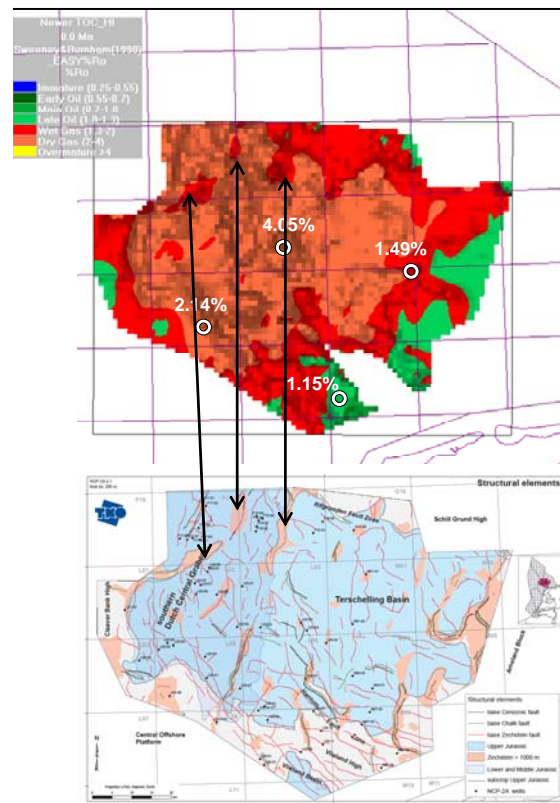
Figure 36. Calculated distribution of present-day maturity of the Ruurlo Formation shows the effect of salt structures: arrows indicate areas with reduced maturities below salt structures.

5.4 Discussion

The 4D basin modelling of the southern part of the Dutch Central Graben and Terschelling Basin provides a comprehensive simulation of many interrelated basinal processes that lead to oil and gas accumulations. Here we used the 4D simulations to increase the process-based understanding of the burial, temperature, maturity and hydrocarbon generation histories of the study area, and to visualize these quantified histories.

Basin modelling results depend on the fulfillment of the limiting assumptions and conditions underlying the approach, the chosen conceptual model of geological evolution of the area and a wide variety of additional input parameters and default relations between lithology and properties (Chapter 2). Here we review some important assumptions and conditions underlying the simulations in the southern part of the Dutch Central Graben and the Terschelling Basin.

We simulated the temperature, maturity and hydrocarbon generation in the study area assuming hydrostatic conditions. In reality large part of the salt-dominated area is highly overpressured (Verweij and Witmans, 2009). Basin modelling programs simulate the temperature evolution using heat flow equations that are based, amongst other things, on lithology- and porosity-dependent thermal conductivities. As a consequence, the temperature evolution and the calculated present-day temperatures and source rock maturation will be affected by the porosity evolution. Hydraulic isolation (e.g. by evaporites) during burial results in overpressuring and undercompaction which is associated with relatively high porosities, and therefore lower thermal conductivities and higher temperatures below the seal in comparison with assumed hydrostatic compaction (Verweij et al., 2007). The 3D basin modelling of the study area assuming hydrodynamic conditions (and disequilibrium compaction) resulted in overestimation of porosities in comparison with measured porosities. The simulated porosities for hydrostatic conditions produced more realistic porosities especially for the highly overpressured sub-salt and Triassic units in the study area. Therefore we decided to use hydrostatic modelling conditions for simulating the temperature and maturity history.

The results of the recently completed detailed mapping of the Terschelling Basin and the southern part of the Dutch Central Graben (Verweij and Witmans, 2009) provided the conceptual model of the geological evolution and the input data and calibration data required for the numerical modelling. The main uncertainties with respect to geological evolution concern the assumed erosional thicknesses, especially of the Upper Germanic Trias Group and the Altena Formation. Increasing or decreasing the original thicknesses of Triassic and Jurassic units may influence the timing and rates of hydrocarbon generation in the Carboniferous source rocks, but not their present-day burial depth and temperatures, and probably have no to only minor influence on their present-day maturities.

Simulation results revealed a marked influence of the Zechstein Group on the distribution of temperatures in the Dutch Central Graben and Terschelling Basin. The lithology assigned to the Zechstein Group is salt. Salt, and also anhydrites have high matrix thermal conductivity in comparison with clastic lithologies. In reality the lithology of the Zechstein Group is not 100% salt. The influence of the Zechstein Group on the simulated temperature distributions presented here can be considered as a maximum influence.

Thermal boundary conditions directly influence the simulation of temperature and maturity history. In this study we applied new, more detailed, basal heat flow boundary conditions and showed the effect on the maturity and hydrocarbon generation history. Later we also also reconstructed new sediment water interface boundary conditions for the Tertiary. The impact of these new boundary conditions on simulation results are published elsewhere (Verweij et al., 2009).

The choice of the kinetic model influence the timing and rates of hydrocarbon generation from source rocks. The effect of using different models was studied in a separate project and will be published separately.

6   Synthesis

The recently in-house gathered, analyzed and mapped data and information on the complex southern part of the Dutch Central Graben and Terschelling Basin were used as input for a full 4D reconstruction of the burial history and history of temperature, source rock maturity and timing of hydrocarbon generation of the study area. The combination of available new data and information and new basal thermal histories, and 4D basin modelling has improved the 4D characterizations and understanding of the burial, thermal and maturity history of the area and provided more detailed information on the timing of the main periods of hydrocarbon generation in the Posidonia Shale and Carboniferous source rocks.

The burial history of the area can be characterized by 3 phases of rapid subsidence and sedimentation that occur in the Dutch Central Graben, Terschelling Basin as well as in the adjacent platform and highs, namely during the Late Carboniferous, Late Permian-Early Triassic (around 270-245 Ma), and Pliocene-Quaternary. An additional Late Jurassic-Early Cretaceous phase of rapid subsidence and sedimentation (154-140 Ma) is apparent in the Graben and even more so in the Terschelling Basin. The Saalian phase of uplift and erosion affected the entire area. A second important phase of uplift and erosion in the Mid Jurassic (appr. 173-154 Ma) is limited to the Terschelling Basin and the platform and highs. A third relatively minor Late Cretaceous phase of uplift and erosion affects the Dutch Central Graben and – the western part of – the Terschelling Basin. The simulated burial, and tectonic subsidence, history showed that the main regional difference between the Dutch Central Graben and Terschelling Basin occurs in Mid-Late Jurassic times. The Carboniferous and Posidonia source rocks are at their maximum depth of burial at present-day.

The 4D simulations indicate that numerous large salt structures of relatively high thermal conductivity had a strong influence on the temperature and maturity history of the area. The salt structures have a 3D effect on heat flow in the subsurface. This is reflected in the significant lateral variations in simulated temperature and maturity at a certain depth.
The 4D modelling results reveal significant lateral variations in maturity and hydrocarbon generation history of each source rock. In addition to the more local influence of salt structures, these variations were found to be related to the structural positions of the source rocks. For example, the Posidonia Shale Formation already starts generating hydrocarbons in Cretaceous times with generation rates reaching their maximum values just before Late Cretaceous uplift west of the inverted centre of the Dutch Central Graben. The generation resumed in Paleogene times and practically stopped at the end of the Paleogene. In contrast, in the inverted centre of the Graben the Posidonia never reached a mature state for hydrocarbon generation. The simulated history of transformation ratios for the Carboniferous source rocks revealed a first phase of hydrocarbon generation before the Mid-Kimmerian uplift in the Terschelling Basin.

A major phase of hydrocarbon generation occurred in both the Graben and the Basin in Latest Jurassic and Early Cretaceous times. There was only limited resumption of hydrocarbon generation in the Graben and a variable resumption of hydrocarbon generation in the Terschelling Basin after the Sub-Hercynian uplift during Paleogene times.

7 References

De Jager, J., 2007. Geological development. In: Wong, Th.E., Batjes, D.A.J. & De Jager, J. (eds): Geology of the Netherlands. Royal Dutch Academy of Arts and Sciences (Amsterdam): p. 5-26.

De Jager, J. & Geluk, M.C., 2007. Petroleum Geology. In: Wong, Th.E., Batjes, D.A.J. & De Jager, J. (eds): Geology of the Netherlands. Royal Dutch Academy of Arts and Sciences (Amsterdam): p. 241 -264.

Duin E.J.T., Doornenbal J.C., Rijkers R.H.B., Verbeek J.W.& Wong Th.E., 2006. Subsurface structure of the Netherlands - results of recent onshore and offshore mapping, Netherlands Journal of Geosciences - Geologie en Mijnbouw, 85-4, pp. 245 - 276.

Geluk, M.C., 2007. Triassic. In: Wong, Th.E., Batjes, D.A.J. & De Jager, J. (eds): Geology of the Netherlands. Royal Dutch Academy of Arts and Sciences (Amsterdam): p. 85-106.

Gradstein, F.M., Ogg, J.G. & Smith, A.G. (eds), 2004. A geologic time scale. Cambridge University Press: 589 pp.

Sweeney, J.J. and Burnham, A.K., 1990. Evaluation of a simple model of vitrinite reflectance based on chemical kinetics. AAPG Bulletin 74, p. 1559-1570.

Sekiguchi, K., 1984. A method for determining terrestrial heat flow in oil basinal areas. In: Cermak, V., Rybach, L., Chapman, D.S. (eds), 1984. Terrestrial heat flow studies of the lithosphere. Tectonophysics 103, 67-79.

Van Adrichem Boogaert, H.A. & Kouwe, W.F.P. (eds), 1993 - 1997. Stratigraphic nomenclature of the Netherlands, revision and update by RGD and NOGEPA, Mededelingen Rijks Geologische Dienst 50.

Van Buggenum, J.M. and Den Hartog, D.G., 2007. Silesian. In: Wong, Th.E., Batjes, D.A.J. & De Jager, J. (eds): Geology of the Netherlands. Royal Dutch Academy of Arts and Sciences (Amsterdam): p. 43-62.

Van Wees, J.D., F. van Bergen, P. David, M. Nepveu, F. Beekman, S. Cloetingh, D. Bonte, 2009. Probabilistic tectonic heat flow modeling for basin maturation: assessment methods and applications. In: Verweij, H., Kacewicz, M., Wendebourg, J., Yardley, G., Cloetingh, S., Düppenbecker, S. (eds.) 2009. Thematic set on Basin Modeling Perspectives, Marine and Petroleum Geology 26, p. 536-551.

Verweij, H., David, P., Souto Carneiro Echternach, M., Bender, A., 2007. Simulation of coupled evolution of pore pressure, fluid flow, compaction and temperature: consequences for correct temperature and maturity prediction in unexplored areas and unconventional basin settings. Poster presented at the AAPG Hedberg Research Conference 'Basin Modeling perspectives: Innovative Developments and Novel Applications', The Hague, Netherlands, 6-9 May 2007.

Verweij, J.M., Souto Carneiro Echternach, M., Witmans, N., Abdul Fattah, R. 2009. Reconstruction of basal heat flow, surface temperature, source rock maturity and hydrocarbon generation in salt-dominated Dutch Basins. AAPG Special Publication on Basin modeling: New horizons in research and applications (submitted).

Waples, D.W. and Waples, J.S., 2004. A review and evaluation of specific heat capacities of rocks, minerals and subsurface fluids. Part 1: Minerals and nonporous rocks. Natural Resources Research 13, 97-122.

Internal TNO reports:
Internal TNO reports and reports by interns and trainees are made available upon request.

Abdul Fattah, R. (trainee, 2007-2008), Van Wees, J-D, Verweij, J.M., Bonte, D. 2008. Tectonic heat flow modelling for the NCP2a area of the Dutch offshore. TNO report 2008-U-R-558/A

Verweij, J.M., and Witmans, N. 2009. Terschelling Basin and southern Dutch Central Graben. Mapping and modeling – Area 2A. TNO Built Environment and Geosciences – National Geological Survey, Utrecht, the Netherlands, TNO report TNO-034-UT-2009-05169.

8   Annex

1. Erosion maps
2. Lithology-related properties and relations
3. Calibration data
4. Burial and thermal history
5. Calibration thermal history
6. Simulated present-day temperature distribution

9   Signature

Utrecht, September 2009   TNO Built Environment and Geosciences

J.C. Doornenbal   J.M. Verweij
Head of department   Author